

Non-adiabatic quantum effects from a Standard Model time-dependent Higgs vev

R. Casadio¹, P. L. Iafelice² and G. P. Vacca³

Dip. di Fisica – Università di Bologna and INFN – Sezione di Bologna,
via Imerio 46, 40126 Bologna, Italy

March 27, 2022

Abstract

We consider the time-dependence of the Higgs vacuum expectation value (vev) given by the dynamics of the Standard Model and study the non-adiabatic production of both bosons and fermions, which is intrinsically non-perturbative. In the Hartree approximation, we analyse the general expressions that describe the dissipative dynamics due to the back-reaction of the produced particles. In particular, we solve numerically some relevant cases for the Standard Model phenomenology in the regime of relatively small oscillations of the Higgs vev.

1 Introduction

In the Standard Model, several fundamental constants such as the Fermi coupling G and the mass of gauge bosons and fermions depend on the vacuum expectation value (vev) of the Higgs field, because of the well-known mechanism of spontaneous symmetry breaking. The equation of motion of the Higgs field on the other hand allows for (periodic) time-dependent solutions for the Higgs vev, which can then be viewed as a particular case of varying fundamental constants (for a review, see Ref. [1]). This behaviour differs from the more common cases of adiabatic variations of the fundamental constants and, due to its periodic nature, can lead to efficient (non-adiabatic) particle production.

The issue of the constancy of the constants of physics was (probably) first addressed by P. A. M. Dirac [2, 3] with his "Large Numbers hypothesis": very large (or small) dimensionless universal constants cannot be pure mathematical numbers and must not occur in the basic laws of physics. He then proposed that they be considered as (typically slowly)

¹email: casadio@bo.infn.it

²email: iafelice@bo.infn.it

³email: vacca@bo.infn.it

variable parameters characterising the state of the Universe and pointed out the possibility of measuring astrophysical quantities to settle this question [4, 5, 6]. More recently, theories such as string theory and models with extra spatial dimensions have also predicted the time-dependence of the phenomenological constants of the low energy regime describing our Universe [7, 8].

The cases we shall consider instead correspond to oscillations of the Higgs vev with periods (set by the Higgs mass scale) of the order of 10^{-26} s. Such a behaviour can be obtained from the usual dynamics of the spatially homogeneous Higgs field [9]. We therefore begin by considering the classical equation of motion for the time-dependent Higgs vev (i.e. a classical condensate) in a homogeneous patch of space-time and identifying the relevant regimes. Quantum fluctuations of fermion and boson fields of the Standard Model are then analysed on this Higgs background and explicit expressions for the particle production [10], an intrinsically non-perturbative effect, are presented. In particular, we investigate which bosons and fermions are produced more abundantly depending on the Higgs mass which we consider in a physically sound range of values [11]. Further, the back-reaction of particle production [12] is analysed in the Hartree approximation which is well suited to describe such a dissipative effect. Similar methods have been previously employed to study particle production in strong fields [13] and pre- as well as re-heating in Cosmology [14, 15, 16].

According to our findings, particle production induced by the oscillating Higgs can be very efficient. From the phenomenological point of view, if the Higgs were oscillating now, the amplitudes of such oscillations should therefore be extremely small. On the other hand, this mechanism could explain how Higgs kinetic and potential energy have dissipated in the past [14]. Note that we typically consider regimes such that only small oscillations around an absolute minimum are present and the symmetry breaking phase transition is not significantly affected. However, since we solve the complete system of coupled non-linear equations that describe particle production and their back-reaction, one does not expect that the produced particles are thermal [17]. They also turn out to have mostly small momenta and are therefore non-relativistic.

In Section 2, we review the solutions of the classical equation of motion for the Higgs vev to properly identify the periodicity properties. Fermion modes on such a Higgs background are then studied in Section 3, with a particular emphasis on the introduction of physical quantities and the regions which lead to quantum particle production. The same kind of analysis is then given for the bosons in Section 4. Fermion and boson production within the Standard Model are then studied in details in Sections 5 and 6, respectively, taking into account the dependence on the Higgs mass. At this stage we neglect the back-reaction. This latter effect, which has to be included to describe consistently the dynamics is then considered in Section 7. In this section we analyze phenomena like the dissipation of the Higgs energy and particle production, consistent with total energy conservation. Final comments are given in Section 8.

We shall use natural units with $\hbar = c = 1$.

2 Higgs vev time dependence

The Higgs sector of the Standard Model Lagrangian we are interested in is given by [18]:

$$\mathcal{L}_H = \partial_\mu H^\dagger \partial^\mu H - \frac{1}{2} (H^\dagger H)^2; \quad (2.1)$$

where H is the complex iso-doublet

$$H = \frac{1}{\sqrt{2}} \exp \left[i \frac{a^a}{v} T^a \right] \begin{pmatrix} v + h(x) \\ 0 \\ 1 \end{pmatrix}; \quad (2.2)$$

(with $a = 1, 2, 3$) are the $SU(2)_L$ generators, a and h (with $\langle h \rangle = 0 = \langle h \rangle$) are scalar fields which parameterise the fluctuations of H around the vacuum state. We have neglected the couplings with gauge and fermion fields.

We find it useful to introduce two new quantities, M_H and β , defined as

$$M_H = \sqrt{2} \frac{M_P}{g}; \quad \beta = \frac{1}{2} M_H^2; \quad (2.3)$$

where g is the $SU(2)_L$ coupling constant and M_H is the "bare" Higgs boson mass (corresponding to constant Higgs vev). In the same way, M is the "bare" weak vector boson mass. The parameter β is such that $\langle h \rangle = 0$ to all orders in perturbation theory. Since we are going to neglect the loop corrections, we set $\beta = 0$ hereafter. Note also that the potential in the Lagrangian (2.1) yields a partial spontaneous symmetry breaking (SSB). In fact, ground-state configurations are only invariant under $U(1)_{em} \times SU(2)_L \times U(1)_\chi$.

The starting point of our work is the assumption that the Higgs field is a time-dependent "classical" homogeneous condensate, $v = v(t)$. Working in the unitary gauge ($a^a = 0$), the Lagrangian (2.1) becomes

$$\mathcal{L}_H = \frac{1}{2} \dot{v}^2 + \frac{M_H^2}{4} v^2 - \frac{1}{8} v^4 + \mathcal{L}_{vh}; \quad (2.4)$$

where a dot denotes the derivative with respect to t and \mathcal{L}_{vh} is a polynomial in h and its derivatives. We then introduce a dimensionless real scalar field ϕ such that

$$v = \sqrt{2} \frac{M}{g} \phi; \quad (2.5)$$

and

$$H = \frac{1}{\sqrt{2}} \begin{pmatrix} \frac{2M}{g} \phi(t) + h(x) \\ 0 \\ 1 \end{pmatrix}; \quad (2.6)$$

in order to study the fluctuations around the constant value $\phi^2 = 1$, which is at the basis of the SSB mechanism. On neglecting all terms involving h (which will be analysed in Section 7), the Euler-Lagrange equation for ϕ becomes

$$\frac{M_H^2}{2} \phi + \frac{M_H^2}{2} \phi^3 = 0; \quad (2.7)$$

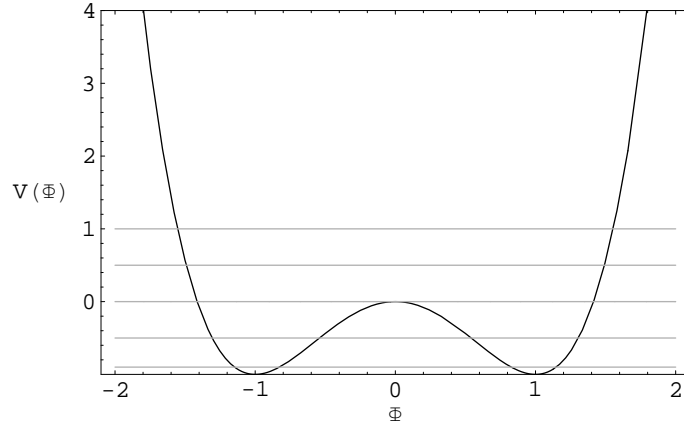


Figure 1: The Higgs vev potential $V(\Phi) = \frac{1}{4}\Phi^4 - \frac{1}{2}\Phi^2$. Straight horizontal lines correspond to $c = 0.9; 0.5; 0.5; 0.1$, with c proportional to the Higgs vacuum total energy.

which can be put in dimensionless form by rescaling the time as $M_H t = 2$ (primes will denote derivatives with respect to τ),

$$\omega^2 - 2(1 - \tau^2) = 0; \quad (2.8)$$

After a simple integration we obtain

$$\omega^2 - 2\tau^2 + \frac{1}{4}\omega^4 + V(\tau) = c; \quad (2.9)$$

where the integration constant $c \in \mathbb{R}$ is a function of the initial conditions. From a physical point of view, c is proportional to the total vacuum energy¹ and $V(\tau)$ is the potential in which this vacuum is "moving" (see g.1).

The equation (2.9) can be formally solved by separating variables, which yields

$$\tau_0 = \int_0^Z \frac{d\tau}{\sqrt{\frac{1}{4} + 2\tau^2 + c}} f(\tau) d\tau; \quad (2.10)$$

Since we are interested in real solutions of Eq. (2.9), we must restrict to the case

$$\frac{1}{4} + 2\tau^2 + c > 0; \quad (2.11)$$

which corresponds to positive kinetic energy for τ (see eq. (2.9)). For any c , the stationary points of $f(\tau)$ are given by $\tau = 0; \pm 1$, for which the potential $V(\tau)$ has a maximum and two minima respectively. Moreover, note that for $c = 0$ and $c = -1$ the integral in Eq. 2.10 is not defined at these points. We shall therefore consider the following cases:

¹It is easy to see that the integral over space of the Hamiltonian density obtained from (2.4) gives the total Higgs vacuum energy $E = M_H c$. We shall thus refer to c as the "Higgs vacuum total energy" for brevity.

1. $c = 1$. Since $c = 1$ corresponds to the absolute minimum in the vacuum total energy, this case is not physically relevant;
2. $-1 < c < 0$. The system exhibits closed trajectories in phase space and a periodic evolution;
3. $c = 0$. The motion is along the separatrix and the system leaves the equilibrium point $\phi = 0$ with an exponentially growing velocity;
4. $c > 0$. The system again exhibits closed trajectories in phase space but with periods longer than those in case 2.

It can further be shown that the solutions for all four cases can be connected by analytic continuation². Therefore, in what follows, we shall use the simplest form of such solutions [20] (which corresponds to $c > 0$) for the sake of simplicity, namely

$$\phi(\eta) = L_m \operatorname{cn}(R_m \eta; m); \quad (2.12)$$

where $L_m = \frac{2}{\sqrt{2m-1}}$ and $R_m = \frac{2}{\sqrt{2m-1}}$. The parameter m is given by

$$m = \frac{1 + \sqrt{1+c}}{2\sqrt{1+c}}; \quad (2.13)$$

and is a function of the initial conditions because so is the vacuum energy c . The function $\operatorname{cn}(z; m)$ is called Jacobi Elliptic function and has the following properties [21]:

$$\text{periods: } 4K; 2K + 2iK' \quad (2.14)$$

$$\text{zeros: } (2l+1)K + 2niK' \quad (2.15)$$

$$\text{poles: } l_n = 2lK + (2n+1)iK'; \quad (2.16)$$

where l, n are integers and $K(m)$ is a special case of the complete elliptic integral of the first kind $F(\phi; m)$,

$$K(m) = F\left(\frac{\pi}{2}; m\right) \quad K^0(m) = F\left(\frac{\pi}{2}; m^0\right); \quad (2.17)$$

with $m^0 = 1 - m$. From (2.14) we deduce that the period along the real (imaginary) axis of the function in Eq. (2.12) is given by

$$T = \begin{cases} \frac{8}{\sqrt{2m-1}} F\left(\frac{\pi}{2}; m\right); & \text{form} < 1 \quad (m > 1) \\ \frac{8}{\sqrt{2m-1}} F\left(\frac{\pi}{2}; m\right) + iF\left(\frac{\pi}{2}; 1-m\right); & \text{form} > 1 \quad (m < 1) \end{cases} \quad (2.18)$$

It is also important to note that the solution (2.12) describes the evolution in time of the Higgs vacuum for every initial conditions $(\phi_0; \dot{\phi}_0)$ only after a suitable time shift (so that $\phi(\eta=0) = 0$).

²These solutions are well known in the literature for the ϕ^4 theory in $(1+1)$ and $(3+1)$ -dimensions [19].

3 Fermions in a time dependent Higgs vev

In the Standard Model the coupling of a generic fermion field to the Higgs scalar field H and gauge fields is described by the Lagrangian density terms [18]

$$\begin{aligned} \mathcal{L}_f = & i \bar{\psi}_L \not{\partial} \psi_L - ig \frac{\tilde{A}}{2} (\bar{\psi}_L \gamma_5 \psi_L) - ig \frac{Y_W}{2} B (\bar{\psi}_L + \psi_R) \gamma_5 \psi_L \\ & + i \bar{\psi}_R \not{\partial} \psi_R - ig \frac{Y_W}{2} B (\bar{\psi}_R - \psi_L) \gamma_5 \psi_R + \bar{\psi}_R G_L H \psi_R + \bar{\psi}_R H^\dagger \psi_L; \end{aligned} \quad (3.1)$$

where ψ_L is a left handed isospin doublet, ψ_R a right handed isospin singlet and G the coupling constant between the Higgs boson and the fermions. Neglecting the gauge fields, in the unitary gauge (2.6), the previous Lagrangian becomes

$$\mathcal{L}_f = i \bar{\psi} \not{\partial} \psi - \frac{G}{2} \frac{2M}{g} (t) \bar{\psi} h(x) \psi; \quad (3.2)$$

with $\psi = \psi_L + \psi_R$. Introducing the "mass parameter"³

$$m_f(t) = \frac{G}{2} \frac{2M}{g} (t) = \frac{G}{2} \frac{M_H}{g} (t) \quad m_f(t); \quad (3.3)$$

with (t) given by Eq. (2.12), the equation of motion for ψ is given by

$$i \not{\partial} \psi - m_f(t) \frac{G}{2} h(x) \psi = 0; \quad (3.4)$$

For our purposes, the last term above can be neglected with respect to the second term proportional to the Higgs condensate and one finally obtains

$$[i \not{\partial} - m_f(t)] \psi(x; t) = 0 \quad (3.5)$$

which is a Dirac equation with a time dependent mass. In a similar manner, one finds that the equation of motion for $\bar{\psi} = \psi^\dagger \gamma^0$ is the Hermitian conjugate of (3.5).

The spinor field is normalized in such a way that $\int d^3x \psi^\dagger(x; t) \psi(x; t) = 1$ and, in the Heisenberg picture, it becomes a field operator with the usual anticommutation rules $\{\psi(x; t), \psi^\dagger(x'; t)\} = \delta^3(x - x')$. We can then expand as

$$\psi(x) = \sum_{s=-\frac{1}{2}}^{\frac{1}{2}} \int \frac{d^3k}{(2\pi)^{3/2}} e^{ik \cdot x} U_s(\vec{k}; t) a_s(\vec{k}) + V_s(\vec{k}; t) b_s^\dagger(-\vec{k}); \quad (3.6)$$

where $s = \pm \frac{1}{2}$ is the helicity,

$$f a_s(\vec{k}); a_{s0}^\dagger(\vec{k}^0) g = f b_s(\vec{k}); b_{s0}^\dagger(\vec{k}^0) g = \delta_{ss^0} \delta^3(\vec{k} - \vec{k}^0) \quad (3.7)$$

³Since there are no stationary states in a time-dependent external field (t) , the mass is strictly speaking ill-defined. We shall however refer to the function $m_f(t)$ as a time dependent mass.

and

$$U_s^Y(\vec{k};t)U_{s^0}(\vec{k};t) = V_s^Y(\vec{k};t)V_{s^0}(\vec{k};t) = \delta_{ss^0} \quad (3.8)$$

$$U_s^Y(\vec{k};t)V_{s^0}(\vec{k};t) = V_s^Y(\vec{k};t)U_{s^0}(\vec{k};t) = 0 ;$$

The vacuum state $|0\rangle$ is as usual defined by the relations

$$a_s(\vec{k})|0\rangle = b_s(\vec{k})|0\rangle = 0 : \quad (3.9)$$

With no time dependence in the theory (i.e., for $m_f(t) = m_f$ constant), $U_s(\vec{k})$ and $V_s(\vec{k})$ would be eigenstates of the operator \vec{k} with eigenvalues m_f and $-m_f$ respectively. The spinors in momentum space $U_s(\vec{k};t)$ and $V_s(\vec{k};t)$ satisfy the charge conjugation relation

$$\mathcal{C}U_s^T(\vec{k};t) = V_s(-\vec{k};t); \quad (3.10)$$

with $\mathcal{C} = i\gamma_0\gamma_2$ ⁴.

It is now convenient to introduce two new scalars defined by

$$\begin{aligned} U_s(\vec{k};t) &= i\gamma_0\gamma_2 + \gamma_3 \sim \vec{k} + m_f(t) \gamma_5 X_k^{(+)}(t) u_s \\ V_s(\vec{k};t) &= i\gamma_0\gamma_2 - \gamma_3 \sim \vec{k} + m_f(t) \gamma_5 X_k^{(-)}(t) v_s; \end{aligned} \quad (3.11)$$

where

$$u_s = \begin{pmatrix} 1 \\ 0 \end{pmatrix}, \quad v_s = \begin{pmatrix} 0 \\ 1 \end{pmatrix}; \quad (3.12)$$

with $\gamma_5 u_s = 1$ and $\gamma_5 v_s = -1$, are eigenvectors of γ_5 with eigenvalues $+1$ and -1 , respectively. Note that $\mathcal{C}u_s^T = v_s$ and Eq. (3.10) is thus identically satisfied. With these notations, Eq. (3.5) yields

$$X_k^{(+)}(t) + \frac{d}{dt} X_k^{(+)}(t) - i m_f(t) X_k^{(+)}(t) = 0; \quad (3.13)$$

which is of the harmonic oscillator type with the complex and (doubly-)periodic frequency

$$\frac{d}{dt} X_k^{(+)}(t) - i m_f(t) X_k^{(+)}(t) = k^2 + m_f^2(t) X_k^{(+)}(t); \quad (3.14)$$

Let us now assume that the Higgs vev remains constant and equal to $v(0)$ for $t \geq 0$. Consequently, the mass $m_f(t)$ will also be constant at negative times and one just has plane

⁴We are using the gamma matrices

$$\gamma_0 = \begin{pmatrix} I & 0 \\ 0 & -I \end{pmatrix}; \quad \gamma_j = \begin{pmatrix} 0 & \sigma_j \\ \sigma_j & 0 \end{pmatrix};$$

where σ_j , $j = 1, 2, 3$ are Pauli matrices and I is the 2×2 identity matrix.

waves for $t = 0$. The evolution for $t > 0$ is then obtained by imposing the following initial conditions at $t = 0^5$

$$\begin{aligned} X_k^{(+)}(0) &= f_2(k)(\epsilon_k(0) + m_f(0))^{1/2} \\ X_{-k}^{(+)}(0) &= i\epsilon_k(0)X_k^{(+)}(0); \end{aligned} \quad (3.15)$$

These together with Eq. (3.13) give

$$X_k^{(+)}(t) = X_k^{(+)}(0) e^{-i\epsilon_k t}; \quad (3.16)$$

so that positive and negative energy modes are not independent and we shall then consider mostly the equation for $X_k^{(+)}$ for simplicity.

It can be showed that if $f_1(t)$ and $f_2(t)$ are two arbitrary solutions of Eq. (3.13) with the sign $(+)$ (or, equivalently, with (i)), the quantity

$$I[f_1; f_2] = \epsilon_k(t)f_1 f_2 + \epsilon_{-k} f_1 f_2 + im_f(t)(f_1 f_2 - f_{-1} f_{-2}) \quad (3.17)$$

is a constant of motion and one can then prove the stability of any arbitrary solutions [22]. Finally, note that if $f_1(t) = f_2(t) = X_k^{(+)}(t)$ the relation (3.17) takes the form

$$X_k^{(+)}{}^2 + \epsilon_k X_k^{(+)}{}^2 + im_f(t) X_k^{(+)} X_{-k}^{(+)} - X_{-k}^{(+)} X_k^{(+)} = 1; \quad (3.18)$$

which is also a consequence of the fact that $U_s(\mathbf{k}; t)$ and $V_s(\mathbf{k}; t)$ are evolved by the Hermitian operators $i^0 @_0 \sim \mathbf{k} m_f(t)$.

3.1 Fermion solutions and physical quantities

The Hamiltonian operator for a fermion field can in general be written as

$$H(t) = i \int d^3x \bar{\psi}(\mathbf{x}; t) \gamma^0 \psi(\mathbf{x}; t); \quad (3.19)$$

Inserting the expansion (3.6) and using Eq. (3.8), this becomes

$$\begin{aligned} H(t) = & \int d^3k \left[\sum_s \left(iU_s^y(\mathbf{k}; t)U_s(\mathbf{k}; t) a_s^y(\mathbf{k})a_s(\mathbf{k}) + iV_s^y(\mathbf{k}; t)V_s(\mathbf{k}; t) b_s(\mathbf{k})b_s^y(\mathbf{k}) \right) \right. \\ & \left. + \sum_s \left(iV_s^y(\mathbf{k}; t)U_s(\mathbf{k}; t) b_s(\mathbf{k})a_s(\mathbf{k}) + iU_s^y(\mathbf{k}; t)V_s(\mathbf{k}; t) a_s^y(\mathbf{k})b_s^y(\mathbf{k}) \right) \right]; \quad (3.20) \end{aligned}$$

⁵We have set the momentum $\mathbf{k} = (0; 0; k)$.

where we have integrated on \mathbf{x} and one of the momenta. Taking into account Eq. (3.11), we end up with

$$H(t) = \sum_{\mathbf{s}} \int d^3k \sum_{\mathbf{k}} \sum_{\mathbf{k}'} \left[E(\mathbf{k};t) a_{\mathbf{s}}^{\dagger}(\mathbf{k}) a_{\mathbf{s}}(\mathbf{k}') + F(\mathbf{k};t) b_{\mathbf{s}}(\mathbf{k}) a_{\mathbf{s}}(\mathbf{k}') + F^*(\mathbf{k};t) a_{\mathbf{s}}^{\dagger}(\mathbf{k}') b_{\mathbf{s}}^{\dagger}(\mathbf{k}) \right]; \quad (3.21)$$

where

$$E(\mathbf{k};t) = \frac{2k^2}{k(t)} \text{Im} \sum_{\mathbf{k}'} X_{\mathbf{k}}^{(+)}(t) X_{\mathbf{k}'}^{(+)}(t) + \frac{m_f(t)}{k(t)}; \quad (3.22)$$

$$F(\mathbf{k};t) = \frac{k}{k(t)} \left(X_{\mathbf{k}}^{(+)}(t) \right)^2 + \frac{2}{k(t)} \left(X_{\mathbf{k}}^{(+)}(t) \right)^2$$

and⁶

$$E^2(\mathbf{k};t) + F^2(\mathbf{k};t) = 1; \quad (3.23)$$

From Eq. (3.22), using (3.15), it is possible to see that $E(\mathbf{k};0) = 1$ and $F(\mathbf{k};0) = 0$, therefore $H(t=0)$ is diagonal. In fact, we have assumed that for $t=0$ the vacuum is constant and there is no explicit time dependence in the theory.

The Hamiltonian (3.21) can be diagonalized at every time using a canonical Bogoliubov transformation [23]. As a matter of fact, the necessary conditions for this kind of diagonalization are ensured by the relations [13]

$$iV_{\mathbf{s}}^{\dagger}(\mathbf{k};t)V_{\mathbf{s}}(\mathbf{k};t) = iU_{\mathbf{s}}^{\dagger}(\mathbf{k};t)U_{\mathbf{s}}(\mathbf{k};t) = k(t)E(\mathbf{k};t) \quad (3.24)$$

$$iU_{\mathbf{s}}^{\dagger}(\mathbf{k};t)V_{\mathbf{s}}(\mathbf{k};t) = iV_{\mathbf{s}}^{\dagger}(\mathbf{k};t)U_{\mathbf{s}}(\mathbf{k};t) = k(t)F(\mathbf{k};t);$$

We now introduce time-dependent creation and annihilation operators,

$$\begin{pmatrix} a_{\mathbf{s}}(\mathbf{k};t) \\ b_{\mathbf{s}}^{\dagger}(\mathbf{k};t) \end{pmatrix} = \begin{pmatrix} k(t) & k(t) \\ k(t) & k(t) \end{pmatrix} \begin{pmatrix} a_{\mathbf{s}}(\mathbf{k}) \\ b_{\mathbf{s}}^{\dagger}(\mathbf{k}) \end{pmatrix} A(\mathbf{k};t); \quad (3.25)$$

and the condition that this be a non singular canonical transformation requires that A is a special unitary matrix,

$$A^{\dagger}(\mathbf{k};t)A(\mathbf{k};t) = 1; \quad (3.26)$$

We have thus shown that $SU(2)$ is the dynamical symmetry group for fermion creation in a homogeneous non stationary scalar field and the time-dependent vacuum $|0_t\rangle$ (see below) is a generalized coherent state built on this group [24].

The hamiltonian also takes the diagonal form

$$H(t) = \sum_{\mathbf{s}} \int d^3k \sum_{\mathbf{k}} \sum_{\mathbf{k}'} \left[E(\mathbf{k};t) a_{\mathbf{s}}^{\dagger}(\mathbf{k};t) a_{\mathbf{s}}(\mathbf{k}';t) + F(\mathbf{k};t) b_{\mathbf{s}}(\mathbf{k};t) a_{\mathbf{s}}^{\dagger}(\mathbf{k}';t) \right]; \quad (3.27)$$

⁶This is a consequence of (3.18).

if the coefficients of the canonical transformation are such that

$$\begin{aligned} j(k;t)^2 &= \frac{1 - E(k;t)}{2} \\ \frac{F(k;t)}{F(k;t)} &= \frac{F(k;t)}{1 - E(k;t)} = \frac{1 + E(k;t)}{F(k;t)}; \end{aligned} \quad (3.28)$$

which are indeed compatible with the condition (3.26) thanks to (3.23).

It is now possible to use the operators a and b to define time-dependent Fock spaces, each of them built from the zero (quasi)particle state at the time t , $a_s(k;t)|0\rangle_t = 0 = b_s(k;t)|0\rangle_t$, which, at $t=0$, are equal to $a_s(k)|0\rangle = 0 = b_s(k)|0\rangle$. These relations mean that a quantized fermion field interacting with a classical external field $\epsilon(t)$ can be represented at every time as a free field, with a corresponding redefinition of the particle concept and vacuum state. Moreover, one can show that diagonalizing the Hamiltonian (3.21) is equivalent to finding exact solutions of the Heisenberg equations of motion and all the matrix elements (expectation values of physical observables) of interest can be written in terms of the coefficients of the Bogoliubov transformation (3.25) [13].

For example, the vacuum expectation value of the (quasi-)particle number operator is given by

$$N_k(t) = \langle 0 | \sum_s b_s^\dagger(k;t) a_s(k;t) | 0 \rangle_t = j(k;t)^2 \langle 0 | \sum_s b_s^\dagger(k) b_s(k) | 0 \rangle = j(k;t)^2 \langle 0 | 0 \rangle; \quad (3.29)$$

where we have used Eqs. (3.25) and (3.9). From the previous relation we see that the number of created (quasi)particle pairs is spin-independent because the homogeneous field is isotropic [25]. If we put the system in a finite volume V , we must replace $|0\rangle$ in (3.29) with $|k\rangle_k = 1$. The (quasi)particle density at the time t is thus given by⁷

$$n(t) = \langle 0 | \frac{1}{V} \sum_s \int \frac{d^3k}{(2\pi)^3} N_k(t) | 0 \rangle_t = \frac{2}{(2\pi)^3} \int d^3k \langle 0 | N_k(t) | 0 \rangle_t = \frac{1}{2} \int dk k^2 j(k;t)^2; \quad (3.30)$$

which is different from zero whenever the Hamiltonian is not diagonal in terms of the operators a and b . The occupation number of fermions created with a given momentum k will be $n_k(t) = j(k;t)^2$, and the condition (3.26) ensures that the Pauli principle is respected at every time [13, 26].

In order to implement numerical methods, it is useful to cast some of the previous expressions in dimensionless form. We thus introduce the following quantities:

$$\frac{M_H}{2} t; \quad \frac{2k}{M_H}; \quad q = \frac{G^2}{2} = 4 \frac{m_f^2}{M_H^2}; \quad (3.31)$$

where $m_f = m_f(\mu = 1) = m_f(0)$. On further multiplying by $4 = M_H^2$, Eq. (3.13) takes the dimensionless form

$$X_k^{(\prime)}{}^{(0)}(\mu) + \mu^2 + q \mu^2(\mu; m) \int_0^1 \bar{q}^{(0)}(\mu; m) X_k^{(\prime)}(\mu) = 0; \quad (3.32)$$

⁷Of course, the same result holds for antifermions.

Moreover, if we define the dimensionless frequency

$$\omega = \frac{2}{M_H} \sqrt{k^2 + q^2}; \quad (3.33)$$

the initial conditions (3.15) become

$$\begin{aligned} X^{(+)}(0) &= \frac{1}{2} [X^{(0)}(0) + \sqrt{q} X^{(0)}(0; m)] \\ \dot{X}^{(+)}(0) &= i X^{(0)}(0) X^{(0)}(0); \end{aligned} \quad (3.34)$$

Note that, despite this is not explicitly indicated, the frequency and the initial conditions are also functions of the amplitude m of the elliptic function, that is of the vacuum energy c (see Eq. (2.13)). On using (3.28), (3.22) and (3.31) we finally obtain

$$n(\omega) = \frac{1}{2} \frac{\text{Im}[X^{(0)}(\omega)]}{\omega} \frac{\sqrt{q}(\omega; m)}{2\omega}; \quad (3.35)$$

which gives the occupation number for every mode ω as a function of the solutions $X^{(\pm)}$ of Eq. (3.32). Analogously, the (dimensionless) energy density will be

$$\rho(\omega) = \frac{1}{2\omega^2} d^2 n(\omega); \quad (3.36)$$

Note that $n(0) = \rho(0) = 0$ thanks to the initial conditions (3.34).

A very useful result follows from the periodicity of the vacuum $\phi(\omega) = \phi(\omega + T)$, which remarkably simplifies the evaluation of the occupation number and shows, although in an approximate way, its explicit time dependence [22]. If we define

$$\omega = \omega(\omega - 1) = \omega(0); \quad (3.37)$$

an approximate expression for $n(\omega)$ is given by¹⁰

$$\hat{n}(\omega) = \frac{1}{2} \frac{\text{Im}[X^{(1)}(T)]^2}{\sin^2(d)} \sin^2 \frac{\omega}{T} F \sin^2(\omega); \quad (3.38)$$

where $X^{(1)}(\omega)$ satisfies Eq. (3.32) with initial conditions $X^{(1)}(0) = 1$, $\dot{X}^{(1)}(0) = 0$ and d is such that $\cos(d) = \text{Re}[X^{(1)}(T)]$. According to Eq. (3.38) the number density of fermions produced depends periodically on ω for all ω . So, on average, this density does not depend on the time during which the external field is turned on. The physical meaning of this result was pointed out by V.S. Popov through a quantum mechanics analogy [22]. Finally observe that in our case the time scale is fixed by the factor $2/M_H$ and if $M_H = 10^2 \text{ GeV}$ then¹¹ $2/M_H = 1.3 \cdot 10^6 \text{ s}$.

⁸This definition is not restrictive since we only need either $X^{(+)}$ or $X^{(-)}$ to calculate $n(\omega)$.

⁹We clearly refer to the period of ϕ along the real axis (see Eq. (2.18)).

¹⁰We shall see in Section 5 that Eq. (3.38) is actually exact at $\omega = nT$ for any positive integer n .

¹¹We recall that $1 \text{ GeV}^{-1} = 6.582 \cdot 10^{25} \text{ s}$ for $\hbar = c = 1$.

3.2 Band structure

A non adiabatic quantum effect arises from the explicit time dependence of the frequency in Eq. (3.32), and this leads to the production of particles. When the time dependence is periodic, one usually speaks of parametric resonance. It is then clear that the quantity q has the role of a resonance parameter due to the fact that the time-dependent terms in Eq. (3.32) are proportional to q .

We are interested in values of q and ω which give solutions of the mode equation associated to particle production, identified by a mean occupation number (see Eq. (3.38))

$$\langle n \rangle = \frac{F}{2} \quad (3.39)$$

different from zero. The result is shown in Fig. 2 in which every peak corresponds to $\langle n \rangle = 1/2$: note the band structure in the plane $(q; \omega^2)$. The left plot in the upper part of Fig. 2 shows the first and second bands while the right plot displays bands from the second to the fourth. Moving along a band, $\langle n \rangle$ oscillates between 0 and $1/2$. Moreover, the bands get narrower with increasing ω^2 for a given value of q and after several bands they shrink to a negligible width, as we show in Fig. 3 with a plot of the mean occupation number as a function of ω^2 for the bottom quark.

To obtain the curves in the lower graphs of Fig. 2 we have studied the mean occupation number along straight lines $\omega^2 = \# q$, with $\#$ constant. First of all, for $\# = 0$ ¹² the peaks are located on the q axis at $q_n (\# = 0) = n^2$, with n a positive integer. We then made the ansatz $q_n (\#) = n^2 (\#)$, with $\omega^2(0) = 1$, for the position of the peaks q_n along the generic line $\omega^2 = \# q$. A numerical interpolation starting from the analysis of the first few peaks for different values of $\#$ has then yielded

$$(\#) = \frac{1}{1 + \#}; \quad (3.40)$$

for which the parametric equation of the lines in Fig. 2 are given by

$$\begin{aligned} \omega^2 &< q_n (\#) = (\#) n^2 \\ &: \quad \omega_n^2 (\#) = \# (\#) n^2; \end{aligned} \quad (3.41)$$

On replacing $\#$ from the first into the second equation, we finally find that the production rate must take its maximum values at points in the plane $(q; \omega^2)$ that satisfy the relation

$$\omega_n^2 + q' = n^2; \quad (3.42)$$

with n a positive integer. Note that the above relation represents a very good approximation in the regime of small oscillations around the static Standard Model Higgs.

The band structure we just described will lead to a preferred production of non-relativistic particles, that is particles with small momentum compared to their mass. For example, for

¹²Note that if $\# = 0$, $\omega^2 = 0$ and $\langle n \rangle = 0$ with no production.

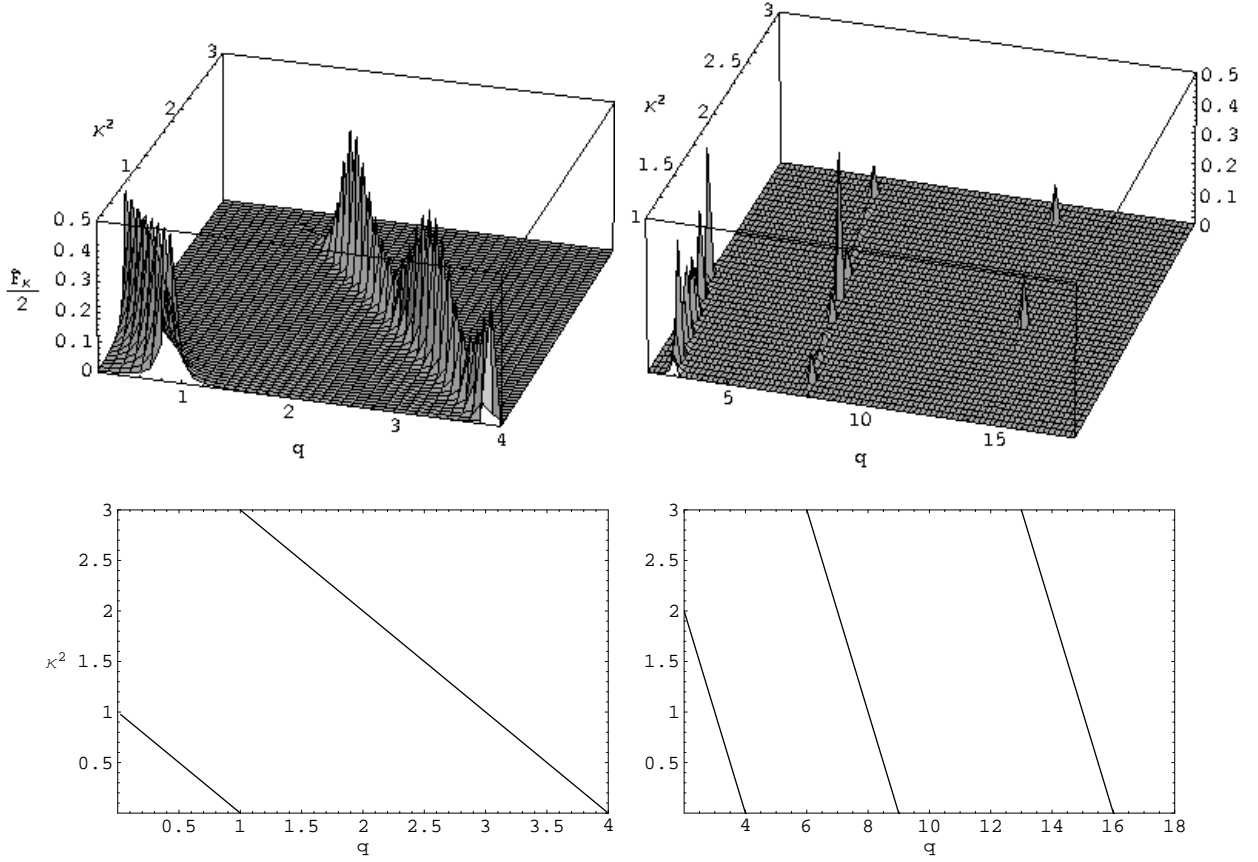


Figure 2: Production chart for fermions coupled to the Higgs. Upper graphs show the occupation number as a function of the parameters q and k^2 . Lower plots show in details the lines in the plane $(q; k^2)$ along which the mean occupation number takes its maximum values. Note that for $\beta \rightarrow 0$ we have $q_n \rightarrow n^2$.

fermions with a mass smaller than $M_H=2$, the production is mostly driven by the first band ($n=1$) and Eq. (3.42) yields a typical momentum $k^2 \approx M_H^2=4 \approx m_f^2$ which is smaller than m_f^2 for the particles we consider in the following. On the other hand, the production of more massive particles will be caused by higher order bands (so that $n^2 - q > 0$) and is normally suppressed.

4 Bosons in a time dependent Higgs vev

The Lagrangian which describes the coupling between the Higgs field and the vector bosons is the same as in Eq.(2.1), but with gauge covariant derivatives and kinetic terms for the gauge fields,

$$\mathcal{L}_{H-B} = D_\mu H^\dagger D^\mu H - \frac{1}{2} H^\dagger H^2 - \frac{1}{4} F_i^{\mu\nu} F_{\mu\nu} - \frac{1}{4} G^{\mu\nu} G_{\mu\nu}; \quad (4.1)$$

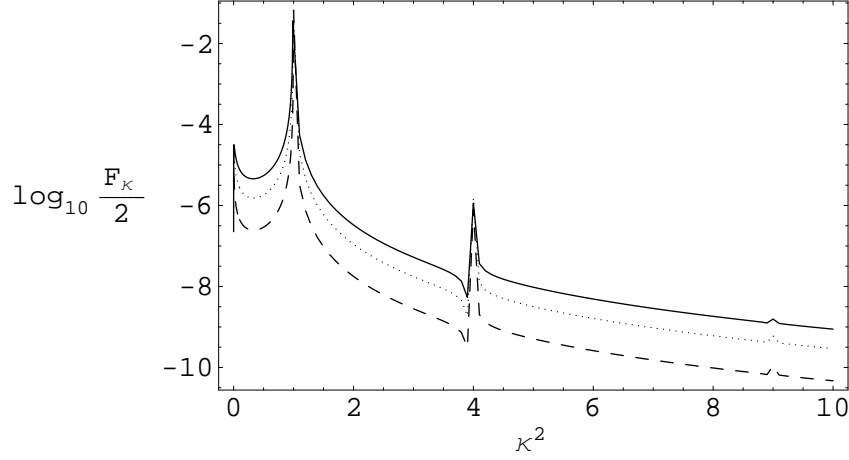


Figure 3: Mean occupation number $F_{\kappa=2}$ as a function of κ^2 for the bottom and $M_H = 115 \text{ GeV}$ (solid line), 200 GeV (dotted line), 500 GeV (dashed line). Note that the peaks get narrower with increasing κ^2 . Similar plots are obtained by varying the resonance parameter q at κ^2 fixed as for decreasing q the bandwidth shrinks.

where $D = \partial_t - i g_2^0 \tilde{A} - \frac{g_2^0}{2} B$, $F^i = \partial_t A^i - \partial_t A^i + g^{ijk} A^j A^k$ and $G = \partial_t B - \partial_t B$. For the electroweak vector bosons we thus have

$$\begin{aligned} L_{W; Z_0} = & \partial_t W^+ \partial_t W - \frac{1}{2} (\partial_t Z)^2 + \frac{g^2}{4M^2} h^2 M^2 W^+ W + \frac{M_Z^2}{2} Z Z + \\ & + \frac{1}{2} M^2 W^+ W + \frac{M_Z^2}{2} Z Z + \frac{g}{M} h M^2 W^+ W + \frac{M_Z^2}{2} Z Z : (4.2) \end{aligned}$$

Taking the vev with the condition $\langle h \rangle = 0$ and neglecting the back-reaction of h , the classical equation of motion for Z is given by

$$\partial_t \partial_t Z + M_Z^2(t) Z = 0; \quad (4.3)$$

The fields W satisfy the same equation with M_Z replaced by M . We therefore conclude that any component \mathcal{Z} of the vector field Z and any component \mathcal{W} of W satisfy Klein-Gordon equations with mass $M_Z^2(t)$, $M_Z^2(t)$ and $M^2(t)$, $M^2(t)$ which, after performing a spatial Fourier transform, take the form

$$\mathcal{Z}_k + k^2 + M_Z^2(t) \mathcal{Z}_k = 0; \quad (4.4)$$

$$\mathcal{W}_k + k^2 + M^2(t) \mathcal{W}_k = 0; \quad (4.5)$$

where $\mathcal{Z}(t) = (2\pi)^{-3/2} \int d^3k e^{i\mathbf{k} \cdot \mathbf{x}} \mathcal{Z}_k(t)$ and $\mathcal{W}(t) = (2\pi)^{-3/2} \int d^3k e^{i\mathbf{k} \cdot \mathbf{x}} \mathcal{W}_k(t)$. Analogously, from the Lagrangian (2.1) in the unitary gauge (2.6) and keeping only terms up to second order, one obtains the following equation for the Fourier modes of the quantum Higgs field

$$h_k + k^2 + M_h^2(t) h_k = 0; \quad (4.6)$$

where

$$M_h^2(t) = M_H^2 \left(\frac{3}{2} \right)^2 (t) - \frac{1}{2} : \quad (4.7)$$

We are interested in the case when the Higgs vev $v(t)$ oscillates near one of its two absolute minima (see Fig. 1). We therefore take the limit $m \rightarrow +1$ ($c \rightarrow 1$) in Eq. 2.12 and obtain

$$(\cdot)' - 1 - \frac{1}{2m} \sin^2 + O\left(\frac{1}{m^2}\right) : \quad (4.8)$$

Moreover, from now on, we shall for simplicity denote with Y any bosonic mode, that is Y can be either \mathcal{Z} , \mathcal{W} or h . Eqs. (4.4), (4.5) and (4.6) then become

$$Y^{(0)}(\cdot) + \mathcal{S}^2(\cdot) Y(\cdot) = 0 ; \quad (4.9)$$

with

$$\mathcal{S}^2(\cdot) = \cdot^2 + q - 1 - \frac{Y}{m} \sin^2 ; \quad (4.10)$$

where we have neglected terms beyond the first order in $1/m$ and introduced the dimensionless constants

$$\frac{2k}{M_H} \quad \text{and} \quad q = 4 \frac{M_Y^2}{M_H^2} ; \quad (4.11)$$

with $M_Y = M_Z, M$ or M_H and $Y = 1$ for the gauge fields and $3=2$ for the Higgs. Note that Eq. (3.32) for the fermion modes takes the same form as Eq. (4.9) when the imaginary part of the fermion frequency can be neglected and that the period of $\mathcal{S}(\cdot)$ is π .

If we define

$$a = \frac{1}{4} h^2 + q - 1 - \frac{Y}{2m} i ; \quad \frac{q_Y}{16m} ; \quad (4.12)$$

and change the time to $\tau = M_H t$, we obtain

$$Y^{(0)}(\cdot) + (a + 2 \cos \cdot) Y(\cdot) = 0 : \quad (4.13)$$

When the total vacuum energy c is near their minimum value $c = -1$ (for which h is constant), W , Z and h therefore satisfy a Mathieu equation.

The Mathieu equation is a linear differential equation with time periodic coefficients and is described in the general framework of Floquet theory [27]. An important result from this theory is the existence of stable solutions only for particular values of a and q (see Fig. 4). For our purposes, the relevant solutions which lead to an efficient particle production in the quantum theory are however those which show an exponential instability of the form $(\cdot)^{(n)}$ (is known as Floquet index or growth factor)

$$Y \sim \exp(\cdot)^{(n)} = 2 \quad (4.14)$$

and appear within the set of resonance bands of width $(\cdot)^{(n)}$ labelled by the integer index n . Using Eq. (4.12) one can then map the stability chart of Fig. 4 into the plane $(q; \cdot^2)$ and finds

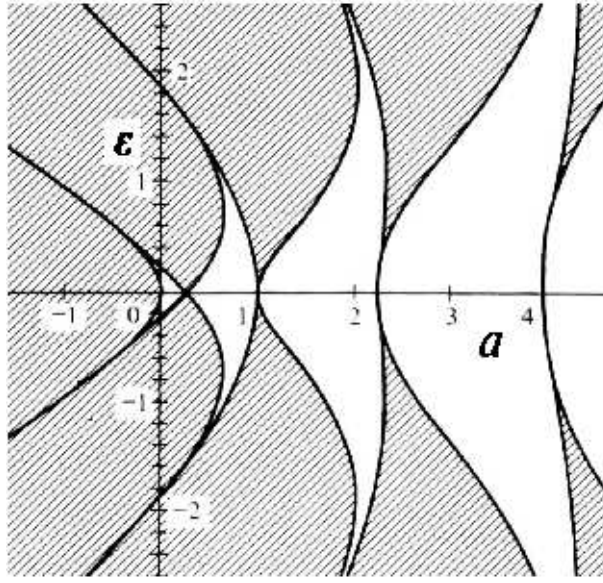


Figure 4: Stability regions for the Mathieu equation. Stable solutions have a and ϵ in the unshaded regions. When $\epsilon = 0$, instability bands cross the a -axis at $a_n = n^2=4$, with $n = 0;1;2;:::$.

that the instabilities also correspond to an exponential growth of the occupation number of quantum fluctuations, $n \sim \exp(\gamma^{(n)})$ (see Eq. (4.18) below), which can be interpreted as strong particle production. Stable solutions also lead to particle production, although with no exponential growth in time, and thus resemble the fermion case [22].

If $c \ll 1$ then $m \ll 1$ and $\epsilon \ll 0$ in Fig. 4. One then finds $4a \approx n^2$, or

$$\frac{q}{n} + q \approx 1 - \frac{y}{2m} = n^2; \quad n = 1;2;3;:::; \quad (4.15)$$

which, for a given q , gives the value of y^2 around which the n -th resonance peak is centred. Further, the physical constraint $y^2 \geq 0$ implies $q \geq 2/m = (2m - 1)$, so if $q \ll 1$ ($M_H \ll 2M_Y$) all the resonance bands contribute to production, otherwise at least the first band ($n = 1$) is not available. In particular, the first band is never available for the Higgs particle and its production can therefore be negligible with respect to that of gauge bosons if the Higgs mass is sufficiently large.

4.1 Boson occupation number and energy density

The same analytical steps of Section 3 allow one to relate relevant physical quantities to the solutions of the equation of motion also in the case of bosons. We again take initial

conditions corresponding to positive frequency plane waves for $\omega > 0$,

$$\begin{aligned} \langle Y^\dagger(0) Y(0) \rangle &= [2\phi(0)]^{-1/2} \\ \dot{Y}(0) &= i\phi(0)Y(0); \end{aligned} \quad (4.16)$$

The occupation numbers for bosons will then be given by [13]

$$n(\omega) = \frac{1}{2\phi} \dot{Y}^{\dagger} \dot{Y} + \frac{\phi}{2} Y^{\dagger} Y = \frac{1}{2}; \quad (4.17)$$

where $\phi = \phi(0)$ and note that $n(0) = 0$ thanks to eqs. (4.16).

Like for fermions, it is possible to find an analytic approximation for the boson occupation number [13],

$$\hat{n} = \sinh^2(\omega T); \quad (4.18)$$

with the Floquet index, or growth factor, T given by

$$\cosh(\omega T) = \text{Re } Y^{(1)}(T); \quad (4.19)$$

in which $Y^{(1)}$ is the solution of Eq. (4.9) with initial conditions $Y^{(1)}(0) = 1$, $\dot{Y}^{(1)}(0) = 0$ and $T = \frac{2\pi}{\omega}$ is the period of $\phi(t)$ (the period of the Higgs vacuum). Using this approximate expression, the boson energy density can be written as

$$\tilde{\rho}_B(\omega) = \frac{1}{2} \int_0^T dt \, \phi^2(t) \sinh^2(\omega t); \quad (4.20)$$

where the tilde on ρ is to remind that this is a dimensionless quantity (like the fermion analogue in Eq. (3.36)).

5 Fermion production

We shall now use the numerical solutions to Eq. (3.32) to evaluate the fermion occupation number n in Eq. (3.35) and compare it with its analytical approximation \hat{n} in Eq. (3.38). In order to illustrate the magnitude of the effect, we shall consider three possible values for the Higgs boson mass which result from different experimental lower or upper bounds, namely $M_H = 115 \text{ GeV}$, 200 GeV and 500 GeV [11]. In this Section, we shall not take into account the back-reaction of the produced fermions which is treated later.

Let us begin with Fig. 5, which shows the time evolution of the occupation number n and its enveloping \hat{n} for the top quark in the case $M_H = 500 \text{ GeV}$ and two different values of the momentum p , and Fig. 6, which shows the same quantities for the bottom quark in the case $M_H = 200 \text{ GeV}$:

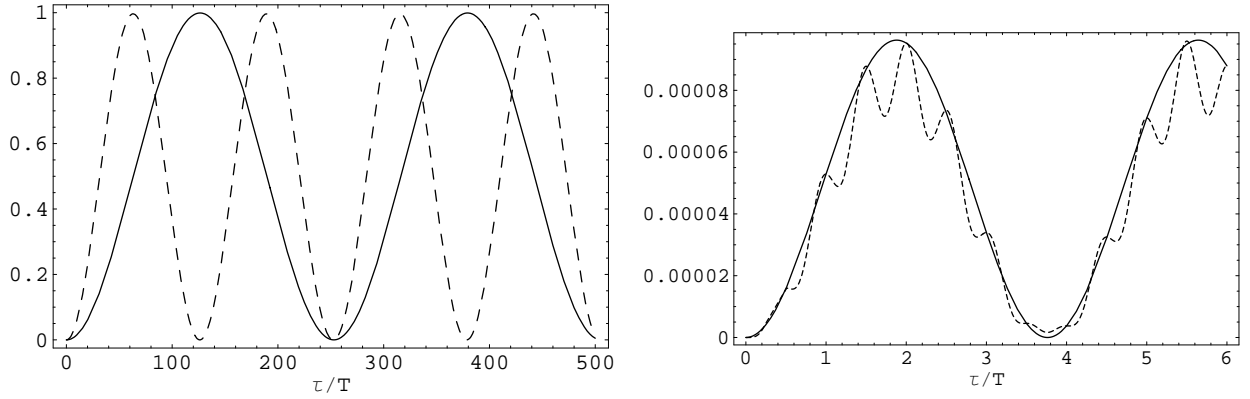


Figure 5: Time evolution of the occupation number n and its envelope \hat{n} for the top quark and $M_H = 500 \text{ GeV}$. Left graph: $\sqrt{s} = 1.4 \text{ TeV}$ on the first resonance band, $c_0 = 1 + 10^{-3}$ (solid line) and $c = 1 + 4 \cdot 10^{-3}$ (dashed line). Note that n and \hat{n} exactly coincide and their period scales as $(c+1)^{1/2}$. Right graph: $\sqrt{s} = 1.4 \text{ TeV}$ is outside resonance bands and \hat{n} (solid line) differs from n (dashed line).

a) For \sqrt{s} on the (first) resonance band both functions n and \hat{n} for the top reach the maximum allowed by the Pauli blocking and are remarkably indistinguishable (left graph in Fig. 5). In fact, their difference remains of the order of 10^{-8} for both values of the initial background energy $c = c(\sqrt{s} = 0)$ and we do not show it. For the bottom (i.e., a smaller value of q at the resonance with respect to the top's) instead, the two functions differ slightly and always remain smaller than one (see Fig. 6). In both cases however, from the numerical simulations one can infer a scaling law for the period T of the occupation number with respect to the initial vacuum energy c . If c_0 is a reference energy, one has

$$T(c) = T(c_0) \frac{c_0 + 1}{c + 1}^{n=2}; \quad (5.1)$$

which holds for all values of \sqrt{s} on the n -th resonance band provided c is small enough that only small oscillation of the background are relevant (see case 2 in Section 2). Note also that $T \propto 1/\sqrt{s}$ for the top (we recall that the Higgs vev period is $2T = M_H^{-1} \approx 10^{-26} \text{ s}$).

b) For values of \sqrt{s} not on a resonance band (right graph in Fig. 5), the production is of course much damped and the exact occupation number shows relatively high frequency oscillations, with period comparable to the Higgs vev's, which are modulated by the function \hat{n} with a period usually larger than T . It is therefore clear that the time average over these relatively high frequency oscillations can still be related to the enveloping \hat{n} as

$$n(\tau) = \langle n(\tau) \rangle + \frac{1}{T} \int_0^{\tau} d\tau' \hat{n}(\tau'); \quad (5.2)$$

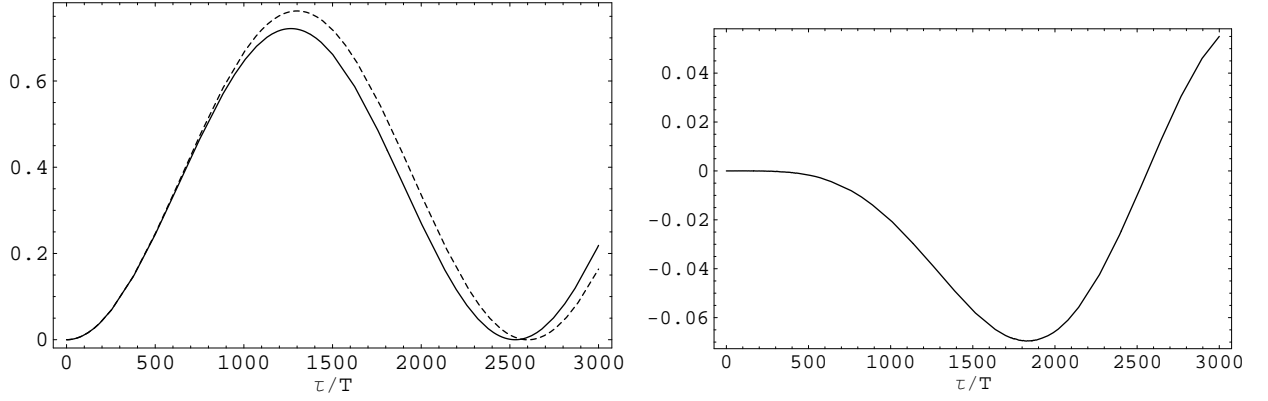


Figure 6: Time evolution of the occupation number for the bottom quark, $M_H = 200 \text{ GeV}$, $\mu^2 = 1$, $q' = 0.9982$ on the first resonance band and $q = 1 + 10^{-3}$. Left graph: n (dashed line) and its envelope \hat{n} (solid line). Right graph: difference between n and \hat{n} .

where \hat{n} is given in Eq. (3.38).

We emphasize that the fermion occupation number is always periodic in time and the function in Eq. (3.38) exactly equals $n(pT)$, with p a positive integer, regardless of the fact that μ and q are on a resonance band or not (see Fig. 5). This is a general behaviour which still holds for very small values of q , for example $q = 10^{-10}$ or $q = 10^{-22}$, corresponding to the scales of the electron and neutrino mass ($\sim 1 \text{ eV}$) respectively. These cases are however very difficult to treat numerically because one should integrate for very long times (the period of the function in Eq. (3.38) grows with the inverse of the fermion mass). For this reason we have chosen to show the occupation number only for quarks like the top and bottom.

We are now interested in the production probability for a given fermion, i.e., in the occupation number n summed over all μ 's for a given value of q (see Eq. (3.31)). The generally oscillating behaviour of n leads us to estimate this probability in time as the mean number (5.2) summed over all the momenta μ ,

$$\langle n \rangle = \int \frac{1}{4\pi^3} d^3p \int_0^Z F \sin^2(\mu p) d\mu = \frac{1}{4\pi^3} \int d^3p \frac{F}{2} : \quad (5.3)$$

As we see from Fig. 3, the mean occupation number $\langle n \rangle$ as a function of q at fixed μ is significantly different from zero only near the values $\mu^2 = \frac{2}{n}$ around which the production peaks are centred. We can therefore estimate $\langle n \rangle$ as

$$\langle n \rangle \approx \frac{1}{4\pi^3} \int_{\text{Supp}(P_n)} d^3p \int_0^Z F \sin^2(\mu p) d\mu \approx \frac{1}{2\pi^2} \int_{\text{Supp}(P_n)} \frac{F}{\mu^2} d^3p \approx \frac{1}{2\pi^2} \int_{\text{Supp}(P_n)} \frac{F}{\mu^2} d^3p \quad (5.4)$$

where $\text{Supp}(P_n)$ is the interval around $\frac{2}{n}$ in which n is significantly large. The effective width of the peak $\frac{2}{n}$ on the n -th band is determined by estimating each integral in the

$M_H = 115 \text{ GeV}$			$M_H = 200 \text{ GeV}$			$M_H = 500 \text{ GeV}$		
	n	q		n	q		n	q
t	10^{-10}	9.26	t	$1.6 \cdot 10^0$	3.06	t	$4.3 \cdot 10^4$	0.48
b	$8.7 \cdot 10^5$	$5.46 \cdot 10^3$	b	$5.1 \cdot 10^5$	$1.80 \cdot 10^3$	b	$2.4 \cdot 10^5$	$2.90 \cdot 10^4$
d	$1.6 \cdot 10^7$	$1.38 \cdot 10^6$	d	$8.2 \cdot 10^6$	$4.54 \cdot 10^3$	d	$3.3 \cdot 10^8$	$7.28 \cdot 10^{10}$
	$3.9 \cdot 10^1$	$9.54 \cdot 10^4$		$2.4 \cdot 10^1$	$3.16 \cdot 10^4$		$8.8 \cdot 10^1$	$5.06 \cdot 10^5$

Table 1: Production probability of various quarks and of the lepton tau for three different values of the Higgs mass and Higgs total vacuum energy $c_0 = 1 + 10^{-3}$.

above expression numerically. Further, we found that

$$n(c)' = n(c_0) \frac{c+1}{c_0+1}^{\frac{n}{2}}; \quad (5.5)$$

a scaling behaviour also shared by the bosons (see Section 6).

The occupation number in Eq. (5.4) for the top, bottom, down and for the tau are shown in Table 1 for three different values of the Higgs mass and Higgs total vacuum energy $c_0 = 1 + 10^{-3}$. Note that the production is mostly generated from the first band and, if $q < 1$, the production probability is larger than for $q > 1$ since for the latter case only the bands of order greater than one can contribute. So, recalling that $q = 4m_f^2/M_H^2$, we conclude that in the Standard Model all the fermions except the top have a greater production probability for a "light" Higgs. Moreover, within a given band, the production is still strongly affected by the resonance parameter q . On varying q along a given band one observes a change in the value of the momentum of the produced particles (see Eq. (3.42)), in the width of the band and, consequently, in the number density of produced particles (see Figs. 2 and 3). These facts lead to the values of n (as defined in Eq. (5.4) above) presented in Table 1. Note finally that the bottom is the "dominant" (with the highest production probability) fermion for $M_H = 115 \text{ GeV}$ and $M_H = 200 \text{ GeV}$, while for $M_H = 500 \text{ GeV}$ the top production is more probable.

We remark that the average occupation number n also scales with the energy according to the relation

$$n(c)' = n(c_0) \frac{1+c}{1+c_0}^{\frac{n}{2}} (1+c)^{\frac{n}{2}}; \quad j+1j \cdot 10^{-3}; \quad (5.6)$$

where n is the order of the "dominant" peak (the one which contributes most to the production). So if one is interested in the production probabilities at an arbitrary but always very small energy, the values in Table 1, calculated for $c_0 = 1 + 10^{-3}$, must be multiplied by the factor $[(1+c)/(1+c_0)]^{\frac{1}{2}}$ if the production is associated with the first band. For example, this is true for the top if $M_H > 2m_{\text{top}}$ and all other fermions for any Higgs mass. Instead, in the region $M_H < 2m_{\text{top}}$ (of phenomenological interest), the top may be produced only starting from the second band and the relevant scale factor is $(1+c)/(1+c_0)$.

Finally, we evaluate the fermion energy density using Eq. (3.36). The integral over \mathbf{k} can be calculated in the same way as in Eq. (5.4) and including just the dominant peak for the production. This approximation is better the lower the Higgs vacuum energy, since the peak amplitude decreases proportionally to this energy. we thus find

$$\rho_f(\mathbf{k}) = \frac{1}{2^3} \int_{\text{Supp}(\mathbb{P}_{\text{dom}})} d^3 \mathbf{k} \left(\frac{F}{2} \sin^2(\mathbf{k} \cdot \mathbf{z}) \right)^n \frac{1}{2^3} \int_{\text{Supp}(\mathbb{P}_{\text{dom}})} d^3 \mathbf{k} \left(\frac{F}{2} \sin^2(\mathbf{k} \cdot \mathbf{z}) \right)^n : \quad (5.7)$$

Around the dominant peaks \mathbf{z}_n given by Eq. (3.42) we have

$$\mathbf{z}_n^2 = 1; \quad (5.8)$$

and we can therefore write the energy density (5.7) as

$$\rho_f(\mathbf{k}) = \frac{\sin^2(\mathbf{k} \cdot \mathbf{z})}{2^3} \int_{\text{Supp}(\mathbb{P}_{\text{dom}})} d^3 \mathbf{k} \left(\frac{F}{2} \sin^2(\mathbf{k} \cdot \mathbf{z}) \right)^n \frac{\sin^2(\mathbf{k} \cdot \mathbf{z})^{X_p}}{2} \frac{1}{2^n} \int_{\text{Supp}(\mathbb{P}_{\text{dom}})} d^3 \mathbf{k} \left(\frac{F}{2} \sin^2(\mathbf{k} \cdot \mathbf{z}) \right)^n; \quad (5.9)$$

which significantly simplifies the evaluation of the integral over \mathbf{k} . One can also find a scaling law for the energy density so obtained, namely

$$\rho_f \sim (1 + c)^{\frac{n}{2}}; \quad (5.10)$$

with the same prescriptions as for n .

From Eq (2.4), the vacuum energy in a volume $8=M_H^3$ can be calculated and put in the usual dimensionless form as

$$\mathbb{E} = \frac{16}{M_H^4} E = \frac{2}{c}; \quad (5.11)$$

The Higgs vacuum energy density available for the production is thus given by

$$\mathbb{E} = \mathbb{E} = \mathbb{E}_{=1} = \frac{2}{c+1}; \quad (5.12)$$

In the Standard Model c appears as an arbitrary parameter and there are presently no experimental constraints on it. There are however good reasons to believe that $c < 1$ but we shall consider in all our calculations simply the value $c = 1$. Taking into account the dependence of $h \sim i$ and \mathbb{E} on c , the fraction of total energy absorbed by a given fermion scales as

$$R(c) = \frac{h \sim i}{\mathbb{E}} = R(c_0; c) = \frac{1 + c_0}{1 + c}^{n=2}; \quad R(c_0; c) = \frac{1}{2} (1 + c_0)^{n=2} h \sim (c_0) i \quad (5.13)$$

An example of this quantity is plotted in Fig. 7. Notably, the maximum value is reached before the end of the first vacuum oscillation.

Using the results shown in the Table 1, for each included fermion we have selected the values of the Higgs mass which give the greatest production probability and the corresponding

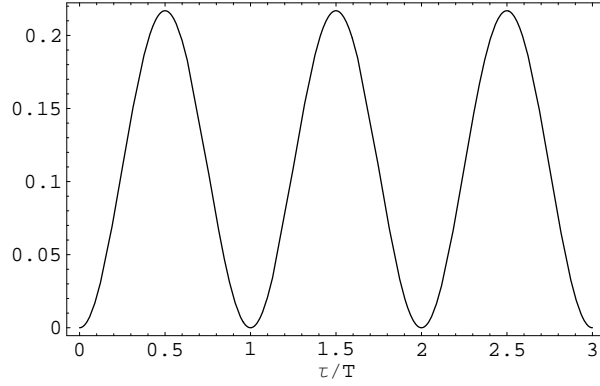


Figure 7: Fraction of Higgs vacuum energy R absorbed by the produced top for $M_H = 500 \text{ GeV}$ and $c_0 = 1 + 10^3$.

	R	q	M_H
t	$1.1 \cdot 10^1$	0.48	500 GeV
b	$2.2 \cdot 10^2$	$5.46 \cdot 10^3$	115 GeV
d	$4.0 \cdot 10^5$	$1.38 \cdot 10^8$	115 GeV
	$1.0 \cdot 10^6$	$9.54 \cdot 10^4$	115 GeV

Table 2: Fraction of Higgs vacuum energy absorbed by various quarks and the tau lepton for the particular Higgs mass (out of the three considered in Table 1 with $c_0 = 1 + 10^3$) which gives the highest production rate.

energy densities are shown in Table 2 in units of the Higgs vacuum energy density available for the production \mathcal{E} . Of course, the physical condition $R < 1$ limits the range of validity of this first approximation where production is not taken to affect the vev oscillation (no back-reaction), breaking energy conservation. For example, the value of R given in Table 2 for the top for $c_0 = 1 + 10^3$ can be rescaled down to a minimum energy $c' = 1 + 4 \cdot 10^4$, for our choice of \mathcal{E} .

When their energy density becomes comparable with the background energy, the produced fermions are expected to back-react on the Higgs vev, thus affecting its evolution and eventually suppressing the parametric production of particles. We shall see this in detail in Section 7. For now we just note that the different scaling law for the top quark energy density as a function of c (when the Higgs mass is large) implies that back-reaction effects will become important sooner and one should therefore be aware that in this case, for very small Higgs energy oscillations, the top energy density produced will be strongly affected by these effects.

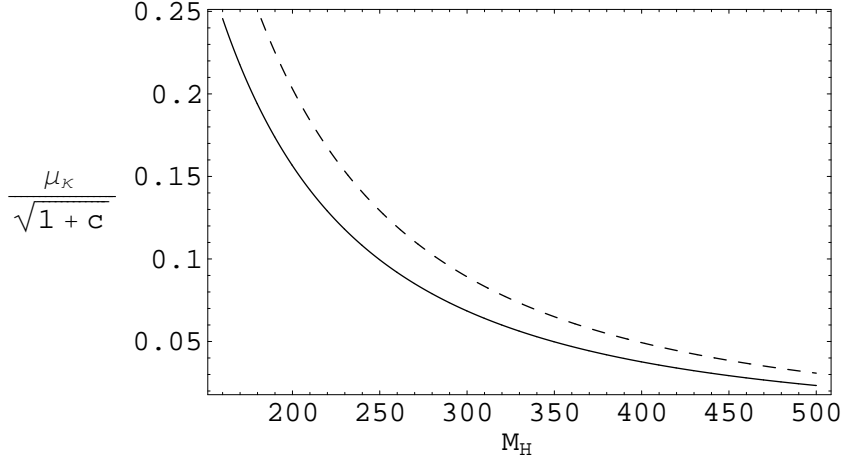


Figure 8: Floquet index for the first resonance band $^{(1)}$ as a function of the Higgs mass for Z^0 (dashed line) and W (solid line). In both cases $^{(1)}$ is maximum if $M_H = 2M_Y$ and decreases for larger values. A factor $\frac{1}{\sqrt{1+c}}$ on the vertical axis is used in consideration of Eq. (6.1) with $c_0 = 1 + 10^{-3}$.

6 Boson production

In Section 4 we reviewed the fact that the equation of motion for a bosonic field admits unstable solutions only for some values of the parameters q and β . The results of the numeric integration of Eq. (4.9) will be used to evaluate the occupation number for every mode n given in Eq. (4.15). For both Z_0 and W we have seen that, for a given value of M_H , the first band ($n = 1$) contributes to the production in an extremely dominant way with respect to the others since the Floquet numbers scale with the Higgs vacuum energy according to

$$^{(n)}(c)' = \frac{1+c}{1+c_0}^{\frac{n}{2}} ^{(n)}(c_0); \quad (6.1)$$

where we usually take $c_0 = 1 + 10^{-3}$. Therefore, in the following we shall just refer to the first band and then do not describe the Higgs production (see Section 4), which could be trivially included. Moreover, motivated by the discussion at the end of Section 4, we shall first study the case $M_H = 2M_{Z^0} = 182 \text{ GeV}$ as the plot in Fig. 8 shows that this yields a more efficient production.

Let us note that for the case of production dominated by the second band (i.e., for bosons with mass less than twice the Higgs mass, including the Higgs itself), the relevant Floquet index is much smaller. In particular, a plot similar to that in Fig. 8 would display a curve for $^{(2)}$, which scales as $(1+c)$ instead of $(1+c)^{1/2}$, with maximum value on the vertical axis of the order of 10^{-2} .

Fig. 9 shows the time dependence of the occupation number (4.17) and its enveloping

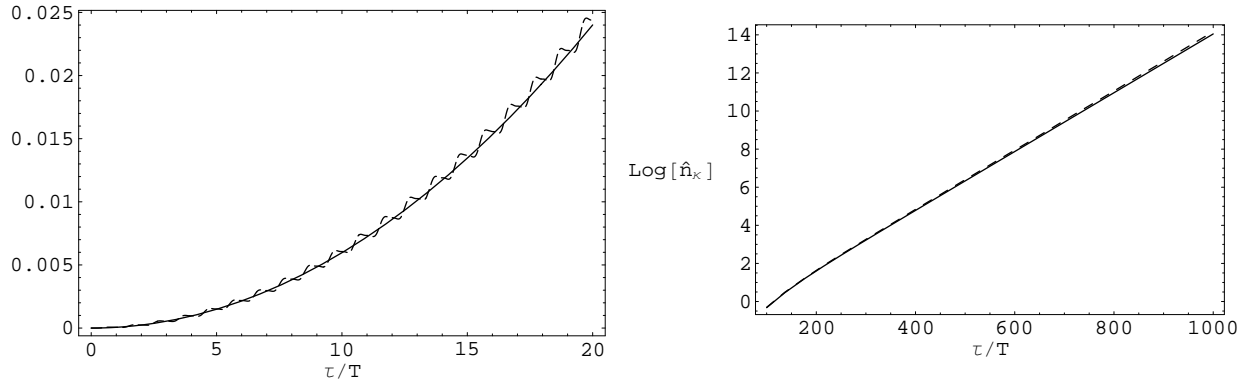


Figure 9: Time evolution of the number of produced Z^0 with $\frac{\omega}{\omega_1} = 0.17$ for two time ranges, $M_H = 200 \text{ GeV}$ and $c_0 = 1 + 10^{-3}$. Note that \hat{n} (solid line) matches n (dashed line) at the end of each background oscillation.

approximation (4.18) for the boson Z^0 with a momentum on the first resonance band, $\frac{\omega}{\omega_1} = 0.17$, $M_H = 200 \text{ GeV}$ and $c_0 = 1 + 10^{-3}$. The exact n , whose mean value grows exponentially with time, oscillates and coincides with \hat{n} at the end of each background oscillation.

To evaluate the production probability (i.e., the total occupation number) for a given boson we must integrate the mode occupation number n over a finite volume in momentum space (at fixed q). This very difficult integration is greatly simplified by the fact that the production only arises around the peaks in the (q, ω) plane, that is for $\frac{\omega}{\omega_1} = \frac{\omega_n}{\omega_1}$ given in Eq. (4.15). Moreover, the production from the first instability band is the most relevant, so that the integration can be consistently restricted to an interval around ω_1 (denoted as $\text{Supp}(\mathcal{P}_1)$, like for fermions),

$$n_B(\omega) = \frac{1}{(2\pi)^3} \int_{\text{Supp}(\mathcal{P}_1)} d^3 \hat{n}(\omega) = \frac{1}{4\pi^2} \int_{\text{Supp}(\mathcal{P}_1)} d^2 p \frac{1}{\omega} \sinh^2(\dots) : \quad (6.2)$$

We shall then consider two different time scales. For short times ($\omega \tau \ll 1$), the above expression can be approximated as

$$n_B(\omega) \approx \frac{1}{2\pi^2} \int_{\text{Supp}(\mathcal{P}_1)} d^2 p \frac{1}{\omega} (\omega \tau)^2 ; \quad (6.3)$$

whereas for long times ($\omega \tau \gg 1$) we shall use

$$n_B(\omega) \approx \frac{1}{8\pi^2} \int_{\text{Supp}(\mathcal{P}_1)} d^2 p \frac{1}{\omega} e^{\omega \tau} : \quad (6.4)$$

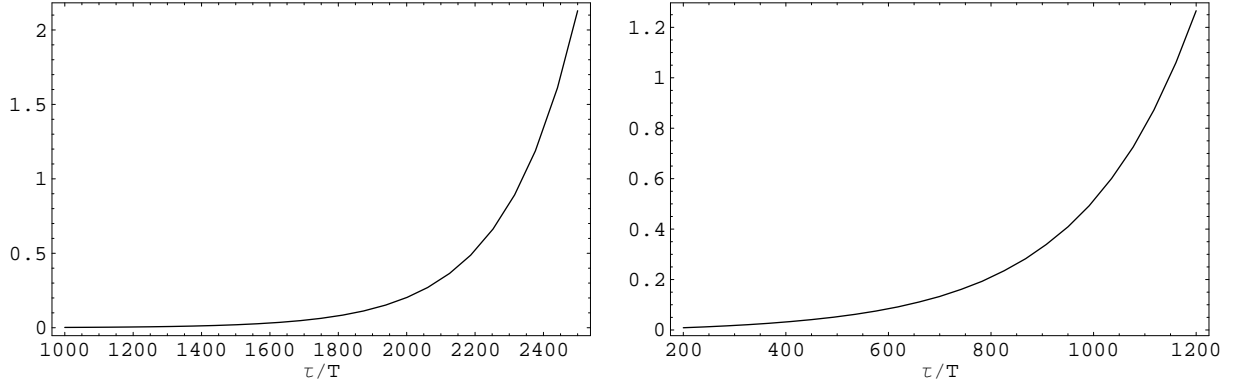


Figure 10: Time evolution of the total number of produced Z^0 (left graph) and fraction of the Higgs vacuum energy absorbed by Z^0 (right graph) for $M_H = 500 \text{ GeV}$ and $c_0 = 1 + 10^{-3}$ (in the right plot, fractions larger than unity signal that the back-reaction cannot be neglected).

The Floquet index as a function of τ^2 has a parabolic shape around τ_1 ,

$$^{(1)} \tau_1^2 = 1 - \frac{\tau_1^2}{2} \tau^2; \quad (6.5)$$

where τ_1^2 denotes the width of the first peak (the same notation we used for the fermions) which scales with the Higgs vacuum total energy exactly according to the same law (5.5) for fermions provided $c_0 = 1 + 10^{-3}$.

For $\tau_1^2 = 1$, the integral in Eq. (6.3) can now be easily estimated and yields

$$n_B(\tau) = \frac{\tau_1^2}{2} N_B(\tau_1^2); \quad (6.6)$$

where $N_B = N_B(\tau_1^2; \tau_1^2)$ is a rather cumbersome expression which we do not show explicitly since it will not be used in the present paper. For long times, one can likewise estimate the integral in Eq. (6.4) using a saddle point approximation and obtain [15]

$$n_B(\tau) = \frac{1}{16} \tau_1^2 \frac{e^{2\tau_1^2}}{\tau_1^2} : \quad (6.7)$$

The left plot in Fig. 10 shows the time dependence of the total number of produced Z^0 following from (6.7) for $M_H = 500 \text{ GeV}$ and $c_0 = 1 + 10^{-3}$. This quantity grows exponentially in time and when the fraction¹³ of Higgs vacuum energy converted into Z^0 approaches unity (see right plot), the back-reaction is expected to become relevant. Indeed, values of that fraction larger than unity do not make sense and actually signal the complete failure of the approximation which neglects the back-reaction. Note that this occurs after

¹³This fraction is defined in analogy with that for the fermions given in Eq. (5.13).

about a thousand background oscillations. Recalling the results for the top from Section 5, it is clear that, during the first few hundreds of vacuum oscillations the energy transferred to the top is larger than that absorbed by the Z^0 , and it seems that the back-reaction of the latter particles can be neglected at an early stage. The production of Z^0 and their interaction with the time dependent Higgs background take the lead later and, with a good approximation, remain the only processes with significant effects (we shall have more to say on this in the next Section).

7 Fermion and boson back-reaction

The results presented so far have been obtained by neglecting the back-reaction of the produced fermions and bosons on the evolution of the Higgs vacuum. This is a common approximation, since a more complete treatment of these effects is a very difficult task. We shall therefore begin by considering the simple case of one kind of fermion simply denoted by ψ (which we shall identify with the top quark later) and one kind of boson (the Z^0).

The Lagrangian density for our system is given by (see Eqs. (2.4), (3.2) and (4.2) with $v = M_H = \frac{1}{\sqrt{2}}v$)

$$\mathcal{L}_{BR} = \mathcal{L}_H - \frac{1}{4} \bar{\psi} \not{\partial} \psi - \frac{1}{8} g_Z^2 Z_\mu Z^\mu; \quad (7.1)$$

where we have redefined the product \hbar to make it dimensionless. The back-reaction effects can be studied to a good degree of accuracy in the Hartree approximation (see Refs. [15, 14] for a discussion on this subject). Let us then consider the vacuum expectation value of the Euler-Lagrange equation for ψ which reads

$$i \not{\partial} \psi - \frac{1}{4} \bar{\psi} \not{\partial} \psi - \frac{1}{4} g_Z^2 Z_\mu Z^\mu \psi = 0; \quad (7.2)$$

The product $\bar{\psi} \not{\partial} \psi$ can be rewritten in terms of an integral in momentum space of the Bogoliubov coefficients (previously introduced to diagonalize the Hamiltonian operator for a generic fermion field) using the expansion (3.6). In this way one encounters ultraviolet divergencies and, in order to obtain a finite result, the operator must be normal ordered to subtract vacuum quantum fluctuations [14, 15, 29]. Moreover, we shall neglect any other renormalization related, for example, to perturbative quantum corrections. Note that after a Bogoliubov transformation the vacuum state $|0\rangle$ is time-dependent and we have a different renormalization at every time. We thus define the (time-dependent) normal ordering of a generic operator as

$$\mathcal{N}(O) = O - \langle 0 | O | 0 \rangle; \quad (7.3)$$

so that the vev of ψ will be given by

$$\begin{aligned} \langle \psi \rangle &= \langle 0 | \mathcal{N}(\psi) | 0 \rangle = \langle 0 | \psi - \langle 0 | \psi | 0 \rangle | 0 \rangle \\ &= \langle 0 | \psi | 0 \rangle - \langle 0 | \psi | 0 \rangle = 0; \end{aligned} \quad (7.4)$$

Using results from Section 3, we find

$$\begin{aligned} h_i &= \int \frac{d^3}{(2\pi)^3} \mathbf{k}^2 \left[\frac{p}{2!} \bar{q}(\mathbf{k}) \right] \frac{1}{2} \\ &= 2n(\mathbf{k}) + \int \frac{d^3}{(2\pi)^3} \mathbf{k}^2 \left[\frac{p}{2!} \bar{q}(\mathbf{k}) \right] \frac{\text{Im} X(\mathbf{k}) X^0(\mathbf{k})}{2!} : \end{aligned} \quad (7.5)$$

As for the Z^0 , analogous prescriptions to those used for the fermion lead to

$$h_{Z^0} = \int \frac{d^3}{(2\pi)^3} \mathbf{k}^2 \left[p \frac{1}{2 + q^2} \right] : \quad (7.6)$$

Note that the two back-reaction terms (7.5) and (7.6) vanish at $t = 0$ by virtue of the initial conditions (3.34) and (4.16), as expected. The system of back-reaction equations is thus

$$\begin{aligned} \ddot{\phi} + 2(1 - \epsilon^2) + \frac{p}{4} \bar{q} h_i - \frac{q}{4} h_{Z^0} &= 0 \\ X'' + (2 + q^2) \frac{p}{4} \bar{q}^0 X &= 0 \\ Y'' + (\epsilon^2 + q^2) Y &= 0 : \end{aligned} \quad (7.7)$$

The last two terms in the first equation (Higgs-fermion and Higgs-vector coupling terms) depend on ϵ , that is the strength of the quartic term in the Higgs vev potential. In the Standard Model the coupling is not fixed but it is possible to take $0 < \epsilon < 1$ if one considers the Higgs self-interaction as described by a perturbative theory.

For the above system, it is easy to show that the (renormalized) total energy

$$E = M_H \left[\frac{c}{2} + \frac{1}{2} \int \frac{d^3}{(2\pi)^3} \left(n^{(f)} + \frac{1}{2} \int \frac{d^3}{(2\pi)^3} \left(n^{(B)} \right) \right) \right] ; \quad (7.8)$$

is exactly conserved by virtue of the equations of motion themselves. In the above

$$c(\mathbf{k}) = \left[\phi^0(\mathbf{k}) \right]^2 - 2\epsilon^2(\mathbf{k}) + \epsilon^4(\mathbf{k}) ; \quad (7.9)$$

the fermion (boson) occupation number $n^{(f)}$ ($n^{(B)}$) and frequency ω (ω) are given in Eq. (3.35) [Eq. (4.17)] and Eq. (3.33) [Eq. (4.10)], respectively.

The approximate evaluation of the integrals (7.5) and (7.6) by restricting their integrand on the dominant band (see also [15]) is based on the results of Sections 5 and 6 for fermions and bosons respectively, and proceeds in a similar way. We therefore assume the validity of scaling laws of the form given, for example, in Eqs. (5.5) or (5.6) and Eqs. (6.6) and (6.7). These approximations are not valid for asymptotically long time evolution, when the dissipative dynamics takes over and very little particle production may still take place. In such a case, one may need different computational schemes, and probably a full lattice approach,

useful also to describe rescattering phenomena and estimate a possible thermalization phase. Nevertheless, our approximation scheme has the virtue of being simple enough to lead to a system of differential equations of finite order which helps to grasp some aspects of the back-reaction dynamics and gains more and more validity in the limit $\beta \rightarrow 1$.

In order to make the qualitative features of the system (7.7) clearer, we shall first study separately its behaviour for short and long times. In particular, as we have seen in the two previous Sections, the production of fermions is expected to dominate during the first few hundreds of Higgs background oscillations and in that regime we shall neglect boson production by simply switching its coupling off and set $M_H = 500 \text{ GeV}$ in order to have the maximum top production. At larger times the production of bosons overcomes that of fermions (limited by Pauli blocking) and we shall then neglect the fermions and set $M_H = 200 \text{ GeV}$ so as to maximize the Z^0 production. In the last Subsection, we shall finally consider the entire system with both the top and Z^0 for $M_H = 500 \text{ GeV}$ in order to show the effect of the fermion back-reaction on the later boson production. This value of the Higgs mass, although not very likely, is chosen as it is particularly convenient to study the interplay between fermion and boson production.

7.1 Fermion back-reaction

As we mentioned above, for relatively short times, we at first consider the evolution of the Higgs background and one fermion, namely the top quark with $M_H = 500 \text{ GeV}$.

The left graph in Fig. 11 shows the time dependence of the corresponding occupation number for the top and Higgs energy densities up to a time $t' = 3.14 \cdot 10^3 T$, where T is the Higgs period without back-reaction) when the boson back-reaction is expected to take over. The Higgs energy oscillates periodically in time and of course takes its minimum values when the top's occupation number is maximum. The right graph displays how the Higgs energy changes in time for different initial values of c , that is for different total energy (all curves assume $\beta = 1$). Note that the maximum fraction of Higgs energy converted into the top increases for decreasing initial total energy, as one would expect from the Pauli blocking. Fig. 12 then compares the top's occupation number with and without back-reaction for $c(0) = 1 + 10^{-5}$. It is clear that the back-reaction in general suppresses the number of produced fermions and this effect is more pronounced for smaller total energy. We also remark that the above numerical solution conserves the total energy with an accuracy better than 1 part in 10^3 .

To conclude this section, we would like to spend a few words about the behaviour of the system with respect to the value of β . Further numerical analysis shows that the fraction of energy absorbed by the produced fermions is proportional to β . Moreover, the system of non-linear differential equations (7.7) seems to produce a chaotic behaviour only for $\beta > 10^6$. In fact for $\beta \leq 10^6$ the highly non-linear term proportional to h^4 becomes of the same order of magnitude as the other terms in the first equation of (7.7). But at this level the approximations used in our equations to evaluate the back-reaction terms should break down.

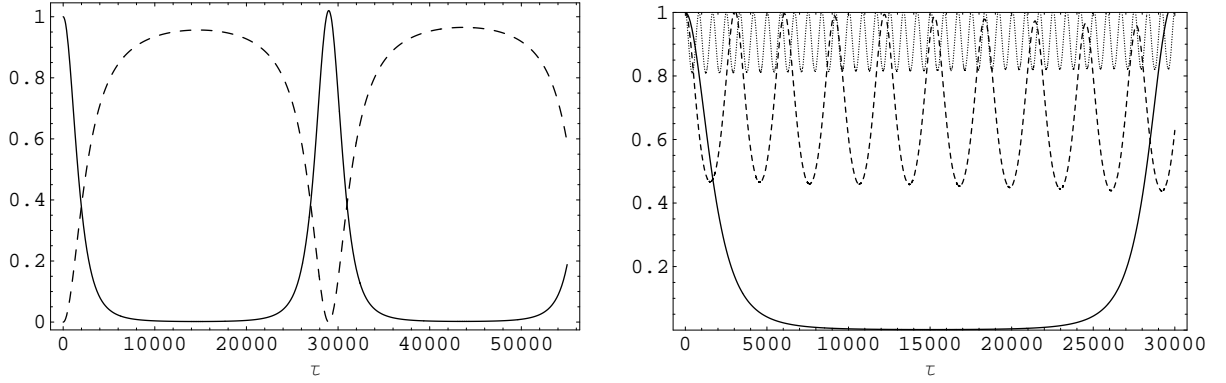


Figure 11: Fermion back-reaction with $M_H = 500 \text{ GeV}$. Left plot: Time evolution of the top occupation number (dashed line) and Higgs vacuum energy (solid line) for $c = 1$ and initial $c(0) = 1 + 10^{-5}$. Right plot: Comparison of the Higgs total vacuum energy for initial values $c(0) + 1 = 10^{-3}$ (dotted line), 10^{-4} (dashed line) and 10^{-5} (solid line). A normalization factor of $[c(0) + 1]^{-1}$ is used for the Higgs energies.

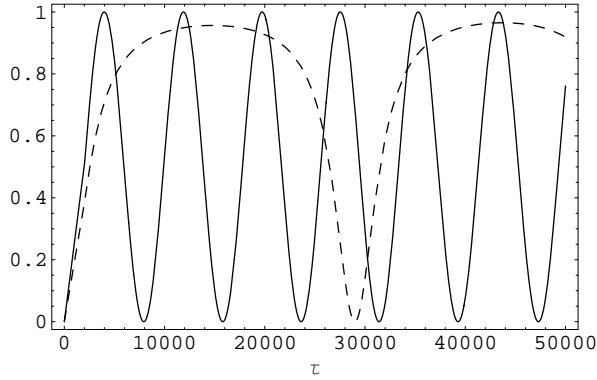


Figure 12: Fermion back-reaction: comparison of top occupation number with (dashed line) and without (solid line) back-reaction for $c(0) = 1 + 10^{-5}$.

7.2 Boson back-reaction

From the results of the previous Section, we know that the energy density of created bosons is comparable to the initial Higgs energy density after about 10^3 vacuum oscillations (that is, for $\tau \approx 3.14 \times 10^3$). The production of bosons then overcomes fermion production (limited by the Pauli principle) and their back-reaction becomes the most relevant phenomenon. We shall therefore neglect the fermion contribution here and just consider the Z^0 and $M_H = 200 \text{ GeV}$ or $M_H = 500 \text{ GeV}$.

Even with the above simplification, it is still very difficult to solve the system (7.7) and we need to employ yet another approximation. Since the integrand in Eq. (7.6) is sharply peaked around the centres of resonance bands, we estimate that integral in the same way we used to obtain the total number of produced bosons in Eq. (6.7), as we have already

anticipated in the general discussion of this Section.

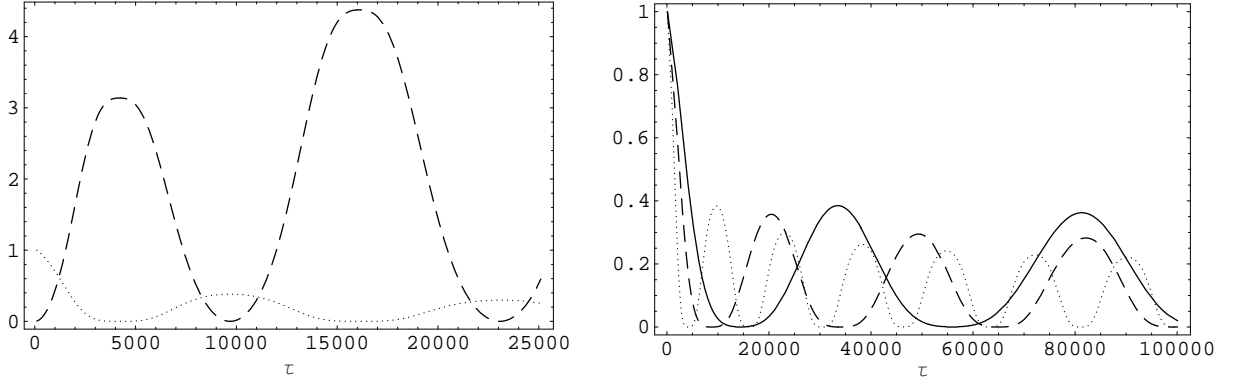


Figure 13: Boson back-reaction with $M_H = 200 \text{ GeV}$. Left graph: Z^0 occupation number (dashed line) and Higgs vacuum energy (dotted line) for an initial value of $c(0) + 1 = 10^5$. Right graph: Time variation of the Higgs vacuum energy for initial total energy $c(0) + 1 = 10^5$ (dotted line), 10^6 (dashed line) and 10^7 (solid line). A normalization factor of $[c(0) + 1]^{-1}$ for the Higgs energies is always used.

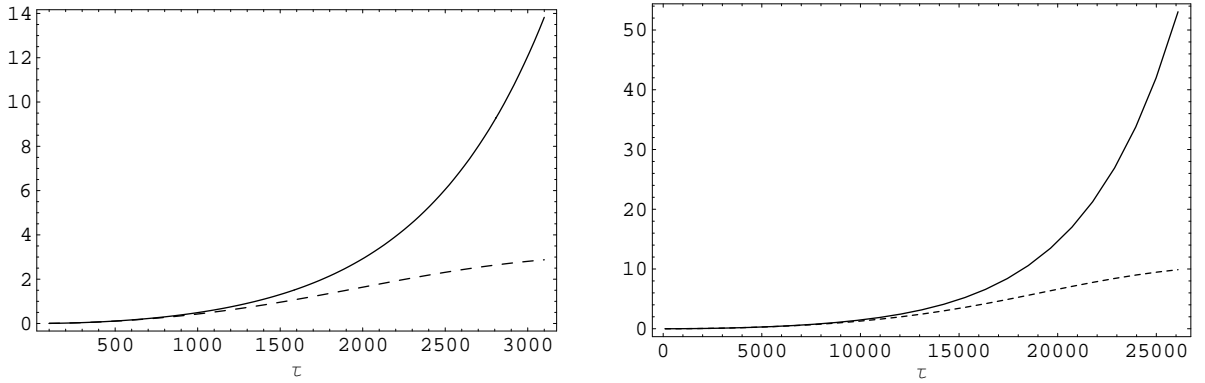


Figure 14: Boson back-reaction: comparison of Z^0 occupation numbers with (dashed line) and without (solid line) back-reaction for $c(0) = 1 + 10^5$. $M_H = 200 \text{ GeV}$ in left plot and $M_H = 500 \text{ GeV}$ in right plot.

We can now solve numerically the system (7.7) and Fig. 13 shows some relevant results. Starting from the left, it is possible to see that the Higgs energy is minimum when the rate of production is maximum. Further, from Fig. 14, one sees that the back-reaction strongly suppresses the boson production. The right plot in Fig. 13 shows the amount of vacuum energy dissipated by back-reaction effects as a function of the time for three different values of the total (dimensionless) energy (which of course coincides with the initial Higgs energy). An important feature of this plot is that we have a "regeneration" of the vacuum energy, which now oscillates in time, and the number of peaks in a given time interval is seen to increase (that is, the periods of oscillations become shorter) for increasing total energy. In all cases, the values at the peaks slowly decrease in time and the periods of oscillations stretch.

One can therefore conclude that the system will evolve towards a complete dissipation of the Higgs oscillations. This is due to the presence of a dumping term [analogous to $1=\bar{p}$ in Eq. (6.7)] that appears in the back-reaction term (7.6) after integrating in .

7.3 Fermion and boson back-reaction

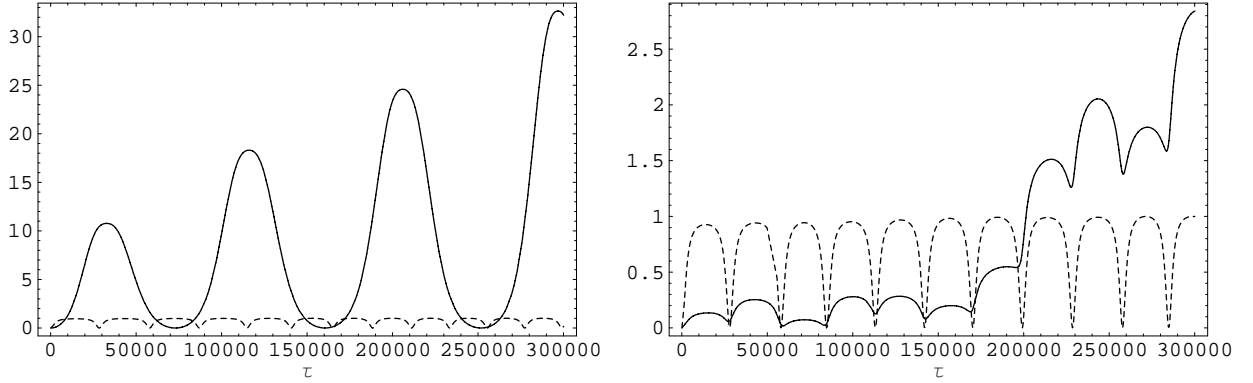


Figure 15: Time evolution of the occupation numbers for the top (dashed line) and Z^0 (solid line) for $\beta = 1, M_H = 500 \text{ GeV}$ and $c(0) = 1 + 10^{-5}$. Left plot: Partial back-reaction from the approximations of Sections 7.1 and 7.2. Right plot: Full back-reaction from Section 7.3.

We finally consider the whole system with the top and Z^0 described by Eq. (7.7) for $M_H = 500 \text{ GeV}$. Again, we choose this value of the Higgs mass in order to have both fermion and boson production from the first resonant band. This corresponds to a particularly complicated scenario with large production of both the top and Z^0 , whereas a more realistic smaller value of M_H would mostly lead to the production of lighter quarks with smaller effects on the Z^0 at late times.

The coupled dynamics is then described in Fig. 15 in which we show on the right the occupation numbers for the top and Z^0 . This results has to be compared to the results of back-reaction computed in the "factorized" approximation used in Secs. 7.1 and 7.2 which we report together for convenience on the left, both computed at $M_H = 500 \text{ GeV}$. We note that the top production is not particularly affected, whereas the Z^0 occupation number is suppressed in the sense that it increases significantly only at later times. The time needed for the production of Z^0 to overtake the top is about one order of magnitude larger than without fermion back-reaction.

As we have already observed, we are able to study the evolution of the system in a window of time far from the asymptotics (presumably with an upper bound in time inversely proportional to β). Beyond that, the adopted approximations break down and the asymptotic time behaviour of the system should be studied taking into account a more accurate description of the mode production (eventually in a full lattice approach) together with the rescattering contribution of the produced particles.

8 Conclusions

We have considered oscillating solutions for the Higgs vev in the context of the Standard Model of particle physics and studied some resulting dissipative effects. In the Standard Model, in fact, the masses of fundamental particles depend on that vev and its oscillations can be viewed as a time-dependent renormalization of the particles' masses which leads to the production of fermion and boson pairs by parametric resonance.

In the first part of the present paper, the back-reaction of the produced pairs has been totally neglected. In this approximation, particle production by the oscillating Higgs appeared to be very efficient. For fermions, the Pauli blocking constrains their occupation numbers to oscillate in time (see Figs. 5) about mean values smaller than one. From the entries given in Table 1, one can see that such mean values strongly depend on the resonance parameter q , that is the Higgs and fermion masses [see the definitions (3.31)]. Moreover, the particular form of the governing Dirac equation (3.13) yields a significant probability of producing only those fermions whose momenta lie on well-defined bands in the $(q; \omega^2)$ -plane [see Fig. 2 and Eq. (3.42)]. Considering the masses of Standard Model particles, this also implies a larger probability of producing fermions with non-relativistic momenta.

As for the bosons, their production is not constrained by any fundamental principles and the governing Mathieu equation (4.13) (in the small oscillation regime) leads to occupation numbers which grow exponentially in time. Analogously to the fermions, the boson production only occurs on narrow bands in the $(q; \omega^2)$ -plane [see the definitions (4.11) and Eq. (4.15)].

In our analysis, we have regarded the Higgs mass M_H as an adjustable parameter, for the experimental data only place a lower bound on it. Consequently, we have given our results for different possible values of M_H and the initial Higgs energy $\phi(0)$ [see the definition (2.9) and Eq. (7.9)]. For natural values of these parameters, we have found that a significant fraction of the initial vacuum energy can be transferred to the fermions before a complete background oscillation (whose period we denoted as T , see Fig. 7). The Pauli blocking then prevents the fermion production from increasing further. The bosons, on the other hand, grow exponentially in time but absorb a significant fraction of the Higgs vacuum energy only after about a thousand oscillations (see Fig. 10). This feature seems to suggest that it is possible to analyse the back-reaction of fermions and bosons separately.

In particular, we have studied the system of one fermion (the top quark) and one boson (the Z^0) coupled to the Higgs field in the Hartree approximation [see Eq. (7.7)]. For such a system, the total energy (7.8) is conserved and, for $0 < \phi(0) < 10^3 T$, the back-reaction of the produced Z^0 has been neglected. To make the problem more tractable, and avoid a complicated study of the system on a lattice of Fourier modes, we have adopted another approximation which might breakdown at asymptotic times. We have thus found that the fermion production is in general mildly suppressed by the back-reaction (see Figs. 11 and 12). At later times ($> 10^3 T$), the back-reaction of the produced top has been neglected and, in the same framework of approximations, we have found that the production of Z^0 is more strongly suppressed by the back-reaction (see Figs. 13 and 14).

The study of the system where both fermion and boson backreaction effects are included has shown a slower boson production, which takes over almost an order of magnitude later in time, against the naive expectation of some kind of factorization in the production events. We however remark that we have chosen a value of the Higgs mass $M_H = 500 \text{ GeV}$ which corresponds to a large production of the top in order to study its effect on the production of the Z^0 . For a more realistic (presumably smaller) value of M_H , one should instead consider the quarks and leptons with the higher production rates (as shown in Table 1).

Future investigations, apart from being focused on more appropriate values of the Higgs mass as, for example, an awaited discovery at LHC would provide, should address aspects which we have found beyond our possibility because of the approximation schemes adopted. In particular, one should investigate the production and dissipative dynamics in the late (asymptotic) times of the evolution and evaluate the rescattering phenomena associated with the produced particles. Keeping in mind that we are mainly considering a possible "starting" regime of very small Higgs oscillations, the rescattering could lead to a thermal background characterized by a very low temperature.

We conclude by noting that, although suppressed when the back-reaction is properly included in the analysis, particle production by parametric resonance with an oscillating Higgs field remains a remarkable effect with phenomenological relevance and could be an (indirect) way of testing the time-dependence of the constants of the Standard Model.

References

- [1] J.-P. Uzan, *Rev. Mod. Phys.* 75, 403 (2003).
- [2] P. A. M. Dirac, *Nature (London)*, 139, 323 (1937); *Proc. Roy. Soc. London A* 165, 198 (1938).
- [3] P. A. M. Dirac, *Proc. Roy. Soc. London A* 338, 439 (1974); *Proc. Roy. Soc. London A* 365, 19 (1979).
- [4] J. Kujat, R. J. Scherrer, *Phys. Rev. D* 62, 023510 (2000).
- [5] S. Hannestad, *Phys. Rev. D* 60, 023515 (1999).
- [6] M. Kaplinghat, R. J. Scherrer e M. S. Turner, *Phys. Rev. D* 60, 023516 (1999).
- [7] T. R. Taylor and G. Veneziano, *Phys. Lett. B* 213, 450 (1988).
- [8] E. Witten, *Phys. Lett. B* 149, 351 (1984).
- [9] G. Passarino, "Are constants constant?," [hep-ph/0108254].
- [10] V. M. Mostepanenko, V. M. Frolov and V. A. Shelyuto, *Yad. Fiz.* 37 (1983) 1261; A. D. Dolgov and D. P. Kirilova, *Sov. J. Nucl. Phys.* 51 (1990) 172 [*Yad. Fiz.* 51 (1990) 273].

- [11] F. Cerutti, in Proc. of the 16th Rencontres de Physique de la Vallée d'Aoste: Results and Perspectives in Particle Physics, La Thuile, Valle d'Aosta, Italia, 3 - 9 Marzo 2002; CERN -ALEPH -PUB -2002 -003. [[hep-ex/0205095](#)];
U. Bauret al., Summary Report of the Precision Measurement Working Group at Snowmass 2001 [[hep-ph/0202001](#)];
Yu. F. Pirogov, O. V. Zenin, Eur. Phys. J. C 10, 629 (1999);
U. Mahanta, "New physics, precision electroweak data and an upper bound on Higgs mass," [[hep-ph/0009096](#)].
- [12] J. Baacke, K. Heitmann and C. Patzold, Phys. Rev. D 58 (1998) 125013.
- [13] V. M. Mostepanenko, A. A. Grib, V. M. Mamayev, Vacuum Quantum Effects in Strong Fields, Friedmann Laboratory Publishing, San Pietroburgo (1994).
- [14] D. Boyanovsky, H. J. de Vega, R. Holman, D. S. Lee and A. Singh, Phys. Rev. D 51 (1995) 4419.
- [15] L. Kofman, A. Linde and A. A. Starobinsky, Phys. Rev. D 56, 3258 (1997).
- [16] J. Garcia-Bellido, S. Mollerach and E. Roulet, JHEP 0002 (2000) 034; P. B. Greene, L. Kofman, A. Linde and A. A. Starobinsky, Phys. Rev. D 56, 6175 (1997); P. B. Greene and L. Kofman, Phys. Lett. B 448 (1999) 6; D. Boyanovsky, H. J. de Vega, R. Holman and J. F. J. Salgado, Phys. Rev. D 54 (1996) 7570.
- [17] D. Boyanovsky, M. D'Attanasio, H. J. de Vega, R. Holman and D. S. Lee, Phys. Rev. D 52 (1995) 6805.
- [18] D. Bardin and C. Passarino, The Standard Model in the making: Precision study of the electroweak interaction, Oxford UK, Clarendon (1999).
- [19] J. A. Espinosa Carrillo, A. J. Maia and V. M. Mostepanenko, Int. J. Mod. Phys. A 15 (2000) 2645.
- [20] I. S. Gradshteyn, I. H. Ryzhik, Table of Integrals, Series and Products, Academic Press, New York (1980). E. T. Whittaker, G. N. Watson, A course of modern analysis, Cambridge Univ. Press (1978).
- [21] R. Erdelyi et al., Higher Transcendental Functions vol. 2, Bateman Manuscript Project, McGraw-Hill (1953);
H. Abramowitz, I. Stegun, Handbook of mathematical functions, Dover (1970).
- [22] V. M. Mostepanenko, V. M. Frolov, Sov. J. Nucl. Phys. 19, 451 (1974).
- [23] N. N. Bogoliubov, Lectures on Quantum Statistics, Kiev: Radjanska Shkola (1949).
- [24] A. M. Perelomov, Theor. and Math. Phys. 16, 852 (1973);
A. M. Perelomov, Theor. and Math. Phys. 19, 368 (1974).

- [25] V . S . Popov, M . S . Marinov, Sov. J. Nucl. Phys. 16, 449 (1973) .
- [26] M . Peloso and L . Sorbo, JHEP 5, 16 (2000) .
- [27] C . M . Bender, S . A . Orszag, Advanced Mathematical Methods for Scientist and Engineer, McGraw Hill (1978) .
- [28] K . Hagiwara et al. (Particle Data Group), Phys. Rev. D 66, 010001 (2002) [URL: <http://pdg.lbl.gov>].
- [29] G . F . Giudice, A . Riotto, I . Tkachev and M . Peloso, JHEP 8, 14 (1999) and references therein .